

# Channel Estimation and Equalization in MultiGigabit Systems

Bernardo Martínez Blas



11

## Index

Introduction .....	5
1. Wireless Channel Characterization.....	7
1.1. Multipath propagation .....	7
1.1.1. Fading.....	7
1.1.2. Intersymbol Interference.....	8
1.2. Frequency selectivity.....	8
1.3. Linear Time Variant Systems .....	11
1.3.1. Stochastic system function .....	14
1.3.2. WSSUS Assumption .....	15
1.3.3. Condensed parameters .....	16
2. Technologies and Physical Layer Modes .....	19
2.1. Technologies.....	19
3. Channel estimation and equalization .....	30
3.1. Data-Aided Equalizers .....	31
3.1.1. Linear Equalizers.....	31
3.1.1.1. Zero Forcing.....	32
3.1.1.2. Minimum Mean Square Error .....	32
3.1.2. Decision Feedback equalizers.....	33
3.1.3. Maximum-likelihood sequence estimator .....	34
3.2. Blind equalizers .....	35
4. Selected Channel estimation and equalization algorithms.....	36
4.1. Channel estimation .....	37
4.1.1. Golay Sequences.....	37
4.1.2. Channel estimation process.....	39
4.2. Zero Forcing Channel Equalization .....	40
4.3. MMSE Channel Equalization.....	41
4.3.1. SNR Estimation .....	41
5. Simulations.....	43
5.1. Simulation System and Scenario .....	43
5.2. Simulation Results .....	53
Conclusions .....	64
References .....	66

## Figure Index

Figure 1. Ellipse model for scattered component with different delays.....	10
Figure 2. Frequency selectivity depending on analyzed channel bandwidth .....	11
Figure 3. Block diagram of a frequency selective and time-variant channel .....	12
Figure 4. Interrelation by the Fourier transform between the four system functions .....	14
Figure 5. Summary of system functions, correlation functions, and special parameters .....	18
Figure 6. OFDM principle.....	20
Figure 7. OFDM transceiver.....	21
Figure 8. SC PHY frame structure .....	22
Figure 9. SC Frame Header structure .....	22
Figure 10. SC PHY Preamble structure.....	23
Figure 11. Sequence value for Golay Sequence a128 and b128 .....	23
Figure 12. Pilot Word structure using data blocks and subblocks .....	24
Figure 13. Sequence value for Golay Sequence a8 and b8 .....	25
Figure 14. Sequence value for Golay Sequence a64 and b64 .....	25
Figure 15. HSI PHY frame structure .....	26
Figure 16. HSI Frame Header structure .....	26
Figure 17. HSI PHY Preamble structure .....	27
Figure 18. PCES positions in the PHY Payload field .....	27
Figure 19. AV HRPDU structure .....	28
Figure 20. AV omni LRPDU structure.....	28
Figure 21. AV directional LRPDU structure.....	28
Figure 22. AV Long omni LRP preamble format.....	29
Figure 23. AV Short omni LRP preamble format.....	29
Figure 24. Decision Feedback Equalizer .....	33
Figure 25. Autocorrelation of Golay Sequence “a” .....	38
Figure 26. Autocorrelation of Golay Sequence “b” .....	38
Figure 27. Sum-Autocorrelation of Golay Sequences “a” and “b” .....	39
Figure 28. System Simulator.....	44
Figure 29. Modulator Bank.....	45
Figure 30. Demodulator Bank .....	46
Figure 31. Amplitude response of raised Cosine with various roll-off factors .....	47
Figure 32. Channel A frequency response .....	50
Figure 33. Channel B frequency response .....	50
Figure 34. Zero Forcing Equalizer with two CES repetitions .....	51
Figure 35. MMSE Equalizer with two CES repetitions .....	52
Figure 36. Channel A: Real channel impulse response .....	53
Figure 37. Channel A: Real channel impulse response VS Estimation with an $E_b/N_0=5\text{dB}$ .....	54
Figure 38. Channel A: Real channel impulse response VS Estimation with an $E_b/N_0=12\text{dB}$ .....	54
Figure 39. Channel A: ZF Equalization VS ZF Equalization with Golay Sequences.....	55
Figure 40. Channel A: ZF Equalization VS MMSE Equalization.....	56

Figure 41. Channel A: BPSK modulation Equalization comparison .....	57
Figure 42. Channel A: QPSK modulation Equalization comparison .....	58
Figure 43. Channel A: 16-QAM modulation Equalization comparison .....	58
Figure 44. Channel B: Real channel impulse response .....	59
Figure 45. Channel B: Real channel impulse response VS Estimation with an $E_b/N_0=5\text{dB}$ .....	59
Figure 46. Channel B: Real channel impulse response VS Estimation with an $E_b/N_0=12\text{dB}$ .....	60
Figure 47. Channel B: ZF Equalization VS ZF Equalization with Golay Sequences .....	60
Figure 48. Channel B: ZF Equalization VS MMSE Equalization .....	61
Figure 49. Channel B: BPSK modulation Equalization comparison .....	62
Figure 50. Channel B: QPSK modulation Equalization comparison.....	63
Figure 51. Channel B: 16-QAM modulation Equalization comparison.....	63

## Introduction

In actual mobile radio systems, multipath conditions pose a problem, as the channel becomes frequency dependent. This point is especially critical in case of high frequency transmissions with very high data rate and high error performance, such as defined in the IEEE 802.15.3c which is an emerging 60-GHz standard supporting data rates of multi-giga bits per second (multi-Gbps) for short-range indoor applications.

The deployment of such high speed wireless transmission has been very difficult throughout history mainly by two critical factors: the first one was the lack of wide enough spectrum and the second one is the high cost of high frequency circuits and devices. However, this trend is changing to the point that not too long ago, the substantial unlicensed spectrum became available at the millimeter-wave band of 60-GHz. Also, the advancement in technology drives the cost of 60-GHz circuits and devices much lower than in the past making possible its use for high definition audio and video wireless transmissions.

In order to overcome the transmission channel issues, it is necessary to include a channel equalizer in the receiver, which must estimate the channel impulse response and make some operations to transform the frequency dependent channel to a flat channel. Nevertheless, the equalizer technology will depend on three different factors: first one the physical layer (PHY) technique under consideration for multi-Gbps Wireless Personal Area Network (WPAN) which basically could be orthogonal frequency division multiplexing (OFDM) or single-carrier frequency domain equalization (SC-FDE); second, the channel impulse response estimation carried out in order to determine the channel transfer function  $H(f)$ , existing several methods to obtain an estimation; and third, the used equalization method and structure in order to reverse all distortions produced by the channel.

This Master thesis has been carry out during an Erasmus program in the *Technische Universität of Braunschweig*, Germany, and it is the first part of a whole European project for the study, analysis and deployment of the IEEE 802.15.3c standard for wireless communications with very high data rate and high error performance in the 60-GHz band. According to the instructions and requirements defined by professor Thomas Kürner which was in charge of this project, this thesis include: first, a theoretical study of all the different propagation effects which could affect a wireless communication channel in order to run not only the simulations presented in this thesis but also the future simulations; second, the development of a model in Matlab/Simulink that will be useful to carry out all the project simulations (taken into account

the specifications collected in IEEE 802.15.3c standard); third, the results of the carried simulations for Single Carrier Channel estimation and equalization by using two different equalization methods in the frequency domain: Zero Forcing and Minimum Mean Square Error equalization.

Taking this into account, the thesis is organized as follows. Section I is dedicated to the study of all the different propagation effects and problems which affects a wireless communication transmissions; In Section II, technologies and Physical Layer Modes are described attending the IEEE 802.15.3c in order to learn its different characteristics for the subsequent channel estimation; Section III is devoted to channel estimation and equalization methods description; estimation and equalization methods are selected in order to carry out the simulations in Section IV; finally, in Section V the developed system simulator as well as the obtained simulation results are presented after implementation of Zero Forcing and Minimum Mean Square Error equalization methods in Matlab/Simulink.

# 1. Wireless Channel Characterization

Wireless communication transmissions present many different features as compared to fixed or wired communication networks. These characteristics are born, on the one hand, from the effects due to the mobility of the system, and on the other hand, due to the specific nature of the medium, the radio channel.

Thus, data transmission between wireless communication systems or devices requires, as a previous and fundamental step, the characterisation of the propagation medium, that is to say, a detailed definition of the factors which affects the radio channel must be done.

In the following sections it will be described all the different phenomenon, effects and problems which have to be considered in order to achieve a successful wireless communication.

## 1.1. Multipath propagation

One of the most important basic phenomenon in wireless communications, and also the catalyst for a lot of effects and problems associated to the radio channel, is multipath propagation.

During a wireless communication, transmitter TX and receiver RX could have a direct connexion between them called Line Of Sight, but normally the signal can get from TX to RX by a lot of different ways or propagation paths, what is called **multipath propagation**. This is due to the numerous Interacting Objects (IOs) that are around the radio channel environment, like for instance, houses, walls, windows or doors which produce reflections or diffractions of the original signal. Each of the received Multi Path Components (MPCs) has different directions of arrival and departure depending on the propagation path, as well as different amplitude, delay and phase shifts between them. Moreover, these MPCs cause effects such as fading or Inter-symbol Interference.

### 1.1.1. Fading

In wireless communications, fading is the deviation that a signal experiences either in amplitude or relative phase of one or more of the frequency components, over certain propagation medium, and usually refers to the attenuation of the signal.

When all the MPCs arrive to the receiver Rx, it process all them together, in other words, it adds them up causing some components to interfere with each other. The interference could be constructive or destructive depending on the phase of the MPCs, and the phase is also related to the propagation way of the component besides the position or possible movement of Rx, Tx or the IOs. This kind of effect is known as small-scale fading or fast fading.

In addition there is also large-scale fading produced by shadowing. It occurs when the LOS component, or any other MPC, is greatly attenuated by an obstacle, preventing the communication between Tx and Rx.

These two types of fading, small and large scale, are combined at the received signal, resulting in a low transmission quality for periods where the signal amplitude is too small. Obviously, this problem leads to high Bit Error Rate (BER), low data rate during transmissions and even to the end of the communication if the quality is really low for a long period of time.

### **1.1.2. Intersymbol Interference**

The different MPCs not only produce fading but also an effect called Intersymbol Interference (ISI). This effect can be easily understood from the interpretation of delay dispersion. Basically, if a symbol time with a length  $T_{SYM}$  is transmitted, the received symbol has a longer duration and therefore interferes with the subsequent symbols.

If no special measures are taken, ISI can lead to errors in the decision device at the receiver that cannot be eliminated by increasing the transmit power. Therefore, when designing the receiver filters, one of the objectives is to minimize the effects of ISI in order to obtain the received data with the smallest error rate. Some ways to ISI include adaptive equalization and error correcting codes.

## **1.2. Frequency selectivity**

Focusing on the current project, that is based on IEEE Std 802.15.3c-2009 [1], it is clear enough that the radio channel has to be modelled as a wideband channel, due to the high data rate and large bandwidth that it is needed in order to broadcast high definition audio and video. Nevertheless the channel behaviour could be different than expected or maybe the frequency selectivity (band type) of the channel it is simply unknown. Thus, in the following lines, it will be explained how to know, in a proper way, the frequency selectivity of the channel and next, it will be described attending to this issue.



As stated before, MPCs not only creates fading but also delay dispersion that can lead to ISI. However, delay dispersion is also an important factor in order to determine which the characterisation of the radio channel is. In fact, there are a set of definitions for commonly used parameters related to delay dispersion that should be useful for a channel characterisation. Some of them are:

- *Excess delay*: The delay of any MPC related to the first one received.
- *Total delay*: The delay difference between the first and the last received component.
- *RMS Delay Spread*: Defined as the root mean square (RMS) of the mean delay as can be seen in the next equation:

$$\tau_{rms} = \sqrt{\frac{1}{\sum_{i=1}^n P_i} \sum_{i=1}^n \tau_i^2 P_i - \left( \frac{\sum_{i=1}^n \tau_i P_i}{\sum_{i=1}^n P_i} \right)^2}$$

where  $P_i = |H_i|^2$  means the delay power spectral density or power delay profile (PDP)  
and  $\tau_i$  means the delay of each “i” Multi Path Component (MPC)

The RMS Delay Spread ( $\tau_{RMS}$ ) is often used as a quantitative criterion for the evaluation of the frequency selectivity of a radio channel, specifically comparing with the symbol interval ( $T_{sym}$ ).

Thus, depending on the criterion, if the delay differences between the scattered received signal components (MPCs) are negligible compared to the symbol interval or  $\tau_{RMS} < T_{sym}$ , then the transmission channel is describe as **not frequency selective**, that is the case of narrowband radio channels. In the other way, the channel is **frequency selective** if the delay differences between MPCs are larger than the symbol interval or  $\tau_{RMS} > T_{sym}$ , affecting the frequency range with strong signal variations within the signal bandwidth, which is the case of wideband transmissions.

The previous concept is also explained by the Parsons’ and Bajwa’s Ellipse Model [2], introducing different zones with the shape of an ellipse where the scattered components of the multipath propagation lead to the same delay dispersion, Figure 1 shows an example.

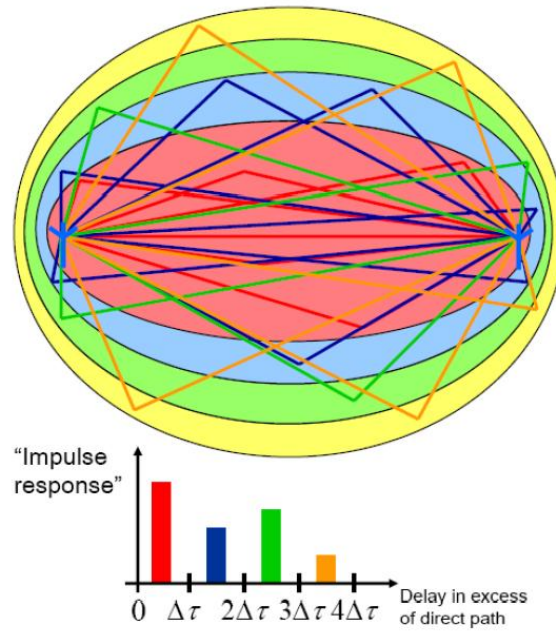


Figure 1. Ellipse model for scattered component with different delays

In this scenario, IOs could be anywhere around the radio channel, however all rays that pass through a specific ellipse arrive at the receiver at the same time, in other words, with the same delay. Then, it is intuitive to say that channel is delay-dispersive if all IOs are not located in the same ellipse, which is the normal case and it is used for modelling wideband channels. Note, that the bandwidth ( $W$ ) of the system will determine if the condition of a single ellipse, non-dispersive channel, it is fulfilled. If a delay  $\Delta\tau$  is lower than the inverse of the system bandwidth ( $\Delta\tau \ll 1/W$ ), the system would not be able to differ between scattered components arriving at  $\tau$  or  $\Delta\tau$ , and it would be considered that all them arrived at the "same time".

The last statement also refers to the fact that the channel frequency selectivity depends on the analyzed bandwidth. In Figure 2, it can be seen that over a large enough bandwidth  $B_2$  the channel will perform a frequency selective response, and with a lower one  $B_1$  a not frequency selective response. In practice, this is the same as compare the maximum delay dispersion of the channel impulse response with the inverse system bandwidth.

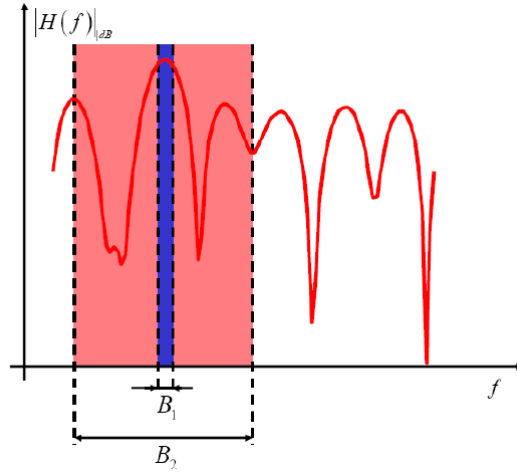


Figure 2. Frequency selectivity depending on analyzed channel bandwidth

To summarize, taking into account all previous considerations, for this project the channel will be modelled as wideband frequency-selective, with a transfer function which varies over the bandwidth of interest due to all the different delays produced by the multipath propagation. This kind of channels involves other characteristics that are defined for Linear Time Variant (LTV) systems, as well as some deterministic approaches that will be carried in the next section.

### 1.3. Linear Time Variant Systems

In order to describe the transfer function of the channel it is necessary to know its behaviour over the time. There are two types of systems, Linear Time Invariant (LTI) and Linear Time Variant (LTV). In LTI systems it is considered that neither transmitter, nor receiver nor IOs change its position over time, they are static, and its impulse response will be defined by  $h(\tau)$ . On the other hand, LTV systems consider that the different MPCs path-lengths between Tx and Rx change with time due to movements in Tx, Rx or IOs, that is what happens in wireless channels. Then, LTV systems have an impulse response  $h(t, \tau)$  that change with time, distinguishing between the absolute time  $t$  and the delay  $\tau$ .

As had been explained before in the Parsons' and Bajwa's Ellipse Model, Figure 1, IOs can be in any place around the plane producing several propagation paths with different delay dispersions. This fact also produces the same effect as if IOs will be moving around, since they are in different ellipses of the radio channel. Then, the impulse response of a wideband channel can be obtained by a time discrete approximation, dividing the impulse response into bins of width  $\Delta\tau$ , which refers to the different propagation delays, and finally computing the sum of them. Figure 3 shows a block diagram of this process where the impulse response of all different delayed components are computed together at the end.

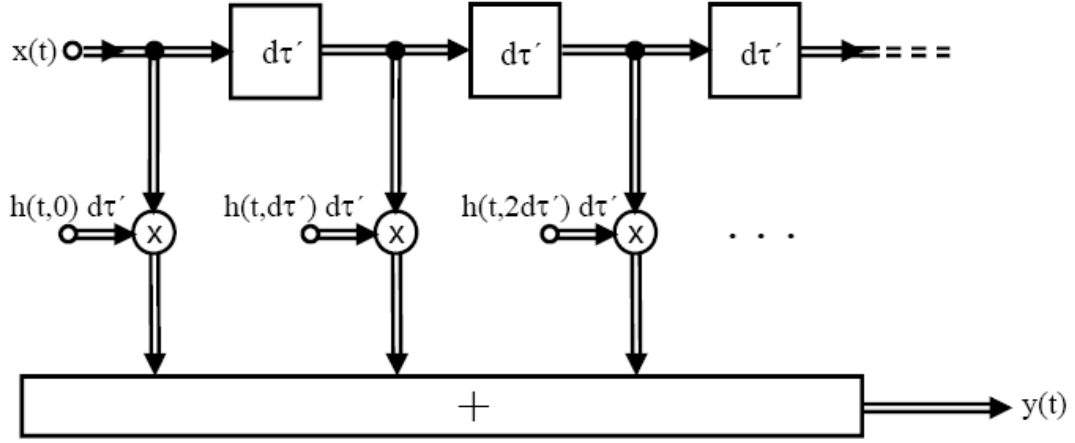


Figure 3. Block diagram of a frequency selective and time-variant channel

Note that due to the causality law, an impulse cannot produce an effect before it has passed through the channel, then the following rule applies:

$$h(t, \tau) = 0 \quad \text{for } \tau < 0$$

Finally the received signal  $y(t)$  for a given input  $x(t)$  will be defined as:

$$y(t) = \int_0^{\infty} x(t - \tau) h(t, \tau) d\tau$$

The *time-variant transfer function*  $H(t, f)$  of the channel is defined by the Fourier transform of the time-variant impulse response  $h(t, \tau)$  with respect to the delay variable  $\tau$ :

$$H(t, f) = \int_0^{\infty} h(t, \tau) e^{-j2\pi f\tau} d\tau$$

In this case, the input-output relationship is defined as:

$$y(t) = \int_{-\infty}^{\infty} X(f) H(t, f) e^{j2\pi f t} df$$

where  $X(f)$  is the Fourier transform of the input signal  $x(t)$ .

It should be mentioned, that neither the time-variant impulse response  $h(t, \tau)$  and nor its corresponding transfer function  $H(t, f)$  allows to know the behaviour of the channel for another typical phenomena in LTV systems, the Doppler effect.

The Doppler effect arises from the movement of Rx and it has a negative influence on the transmission characteristics of the radio channel causing a frequency shift on each of the

received signals components MPCs. The *angle of arrival* ( $\alpha_n$ ), which is defined by the direction of the received MPC and the direction of motion of Rx, determines the *Doppler frequency* or *Doppler shift*  $\nu$  of a particular propagation component according to:

$$\nu = f_{max} \alpha_n$$

Being  $f_{max}$  the *maximum Doppler frequency* related to the speed of the receiver  $V$ , the speed of light  $c_o$  and the carrier frequency  $f_o$ , by the following equation:

$$f_{max} = \frac{V}{c_o} f_o$$

Due to the Doppler effect, the spectrum of the transmitted signal undergoes a frequency expansion during transmission, an effect called *frequency dispersion*, which in the time domain implicates that the impulse response of the channel becomes time-variant.

Applying the Fourier transform on  $h(t, \tau)$  with respect to the time variable  $t$  leads to a different representation called the *Doppler variant impulse response* or the *delay Doppler function*, obtaining an insight of the Doppler effect in the radio channel:

$$s(\nu, \tau) = \int_{-\infty}^{\infty} h(t, \tau) e^{-j2\pi\nu t} dt$$

This *Doppler-variant impulse response* leads to the physical interpretation of the ellipses model of figure X.X, and explicitly describes the dispersive behaviour of the radio channel as a function of both the propagation delays  $\tau$  and the Doppler frequencies  $\nu$ .

Thus, the relation of the input and output signal can be calculated also as:

$$y(t) = \int_0^{\infty} \int_{-\infty}^{\infty} x(t - \tau) s(\nu, \tau) e^{j2\pi\nu t} d\nu d\tau$$

As can be deduced, this relation shows that the output signal  $y(t)$  can be represented by an infinite sum of delayed, weighted, and Doppler shifted replicas of the input signal  $x(t)$ . Signals affected by a Doppler shift in the range of  $[\nu, \nu + d\nu]$  and delayed during transmission between  $[\tau, \tau + d\tau]$  will have a weight of  $s(\nu, \tau) d\nu d\tau$ .

Finally, if the function  $s(\nu, \tau)$  is transformed with respect to the variable  $\tau$ , the resulting function is the *Doppler-variant transfer function*:

$$B(v, f) = \int_{-\infty}^{\infty} s(v, \tau) e^{-j2\pi f\tau} d\tau$$

This equation establishes that the spectrum of the output signal can be understood as a superposition of infinite number of Doppler shifted and filtered replicas of the input signal spectrum.

Summarizing, the deterministic behaviour of a wideband channel can be represented in many different ways attending to the system functions. Next figure 4 shows the interrelation by the Fourier transform between the four system functions presented above.

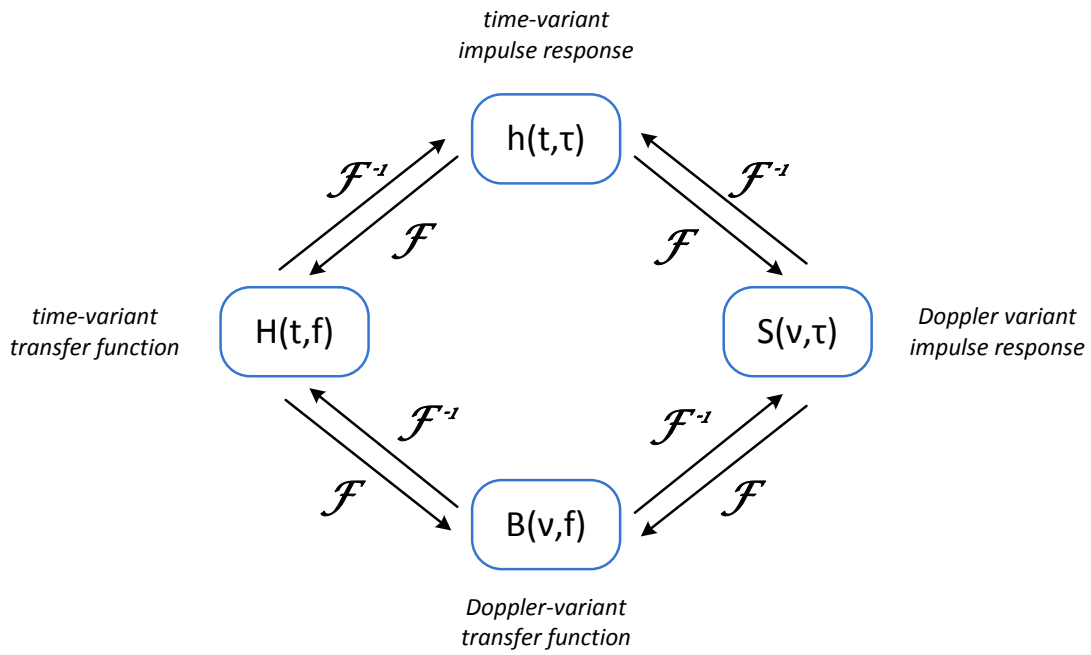


Figure 4. Interrelation by the Fourier transform between the four system functions

### 1.3.1. Stochastic system function

Up to now, it was analyzed the deterministic behaviour of the channel, but the channel can also be studied as a stochastic system. In the following, it will be considered the stochastic behaviour of the channel. In this case, the four functions  $h(t, \tau)$ ,  $H(t, f)$ ,  $s(v, \tau)$ , and  $B(v, f)$  are stochastic system functions, which can be described by the following autocorrelation functions:

$$R_h(t, t', \tau, \tau') = E\{h^*(t, \tau)h(t', \tau')\}$$

$$R_H(t, t', f, f') = E\{H^*(t, f)H(t', f')\}$$

$$R_s(v, v', \tau, \tau') = E\{s^*(v, \tau)s(v', \tau')\}$$

$$R_B(v, v', f, f') = E\{B^*(v, f)B(v', f')\}$$

However, these correlation functions depend on four variables, and are a rather complicated way for the characterization of the channel. Further assumptions about the physics of the channel can lead to a simplification of these functions.

### 1.3.2. WSSUS Assumption

The most important class of stochastic time-variant linear channel models is represented by belonging to the class of WSS models as well as to the US class. These channel models represent wide-sense stationary impulse responses and uncorrelated scattering components respectively, and when applied simultaneously in a channel model are called WSSUS. Due to their simplicity, they are of great practical importance and are nowadays almost exclusively employed for modelling frequency-selective mobile radio channels.

On the one hand, the mathematical definition of wide-sense stationary (WSS) is that the autocorrelation function depends on the difference between two variables, for example  $t - t'$ , instead on the two variables  $t$  and  $t'$  separately. Thus, second order amplitude statistics do not change with time, and the autocorrelation functions can be rewritten as:

$$R_h(t, t', \tau, \tau') = R_h(t, t + \Delta t, \tau, \tau') = R_h(\Delta t, \tau, \tau')$$

On the other hand, the uncorrelated scatterers (U.S.) assumption is defined in this way: “contributions with different delays are uncorrelated”, which is interpreted mathematically to the correlations functions as follows:

$$R_h(t, t', \tau, \tau') = P_h(t, t', \tau)\delta(\tau - \tau')$$

Then, applying both assumptions together to all the correlation functions, it results in the following restrictions:

$$\begin{aligned} R_h(t, t + \Delta t, \tau, \tau') &= \delta(\tau - \tau')P_h(\Delta t, \tau) \\ R_H(t, t + \Delta t, f, f + \Delta f) &= R_H(\Delta t, \Delta f) \\ R_s(v, v', \tau, \tau') &= \delta(v - v')\delta(\tau - \tau')P_s(v, \tau) \\ R_B(v, v', f, f + \Delta f) &= \delta(v - v')P_B(v, \Delta f) \end{aligned}$$

Where the different resulting functions define:

- $P_h(\Delta t, \tau)$ : delay cross power spectral density
- $R_H(\Delta t, \Delta f)$ : time-frequency correlation function
- $P_s(v, \tau)$ : scattering function

- $P_B(v, \Delta f)$ : Doppler cross power spectral density

These expressions are easier to understand because they have two variables instead of the four of the previous correlations functions. However, it would be better a function of one variable or just a parameter for representation as would be shown in the following section.

### 1.3.3. Condensed parameters

To obtain a function of just one variable or parameter, it could be achieved by integrating the previous functions over one of the two variables. For example, integrating the scattering function  $P_s(v, \tau)$  over the Doppler shift  $v$  gives the **Power Delay Profile**  $P_h(\tau)$ , which gives information about how much power arrives at the receiver with a delay between  $[\tau, \tau + d\tau]$ . The Power Delay Profile can also be obtained as:

$$P_h(\tau) = \int_{-\infty}^{\infty} |h(t, \tau)|^2 dt$$

Analogously, integrating the scattering function over  $\tau$  results in the **Doppler power spectral density**  $P_B(v)$ .

Then, by setting  $\Delta t = 0$  from the time-frequency correlation function, it can be obtained also the **frequency correlation function**  $R_H(0, \Delta f)$  which is the Fourier transform of the Power Delay Profile defined before. Analogously, the **temporal correlation function**  $R_H(\Delta t, 0)$  can be obtained by setting  $\Delta f = 0$  to the time-frequency correlation function, being also the Fourier transform of the Doppler power spectral density.

### Power delay profile moments

Finally, to have a quick understand of the measurement results, it is better to obtain only singles parameters instead of functions, this is possible by normalizing moments of the Power Delay Profile. The zero-order moment defines  $P_m$ , the first-order moment normalized will give information about the **mean delay** and the second-order the **RMS delay spread**, as can be seen:

$$P_m = \int_{-\infty}^{\infty} P_h(\tau) d\tau$$

$$T_m = \frac{\int_{-\infty}^{\infty} P_h(\tau) \tau d\tau}{P_m}$$



$$S_T = \sqrt{\frac{\int_{-\infty}^{\infty} P_h(\tau) \tau^2 d\tau}{P_m}} - T_m^2$$

### *Doppler spectra moments*

The same could be applied to the moments of the Doppler spectra for a better understanding of the results. Thus, in analogy to the Power Delay Profile moments, the integrated power  $P_{B,m}$  the **mean Doppler shift**  $v_m$  and the **RMS Doppler spread**  $S_v$ , are defined by the following equations:

$$P_{B,m} = \int_{-\infty}^{\infty} P_B(v) dv$$

$$v_m = \frac{\int_{-\infty}^{\infty} P_B(v) v dv}{P_m}$$

$$S_v = \sqrt{\frac{\int_{-\infty}^{\infty} P_B(v) v^2 dv}{P_{B,m}}} - v_m^2$$

### *Coherence bandwidth and coherence time*

As have been explained, the different frequency components of a frequency-selective channel fade differently. As can be deduced, the correlation between fading at two different frequencies is the smaller the more these two frequencies are separated. The **coherence bandwidth**  $B_{coh}$  defines the frequency range that is required so that the correlation coefficient is smaller than a given threshold.

Assuming WSSUS, the mathematical definition of the coherence bandwidth, in terms of the frequency correlation function  $R_H(0, \Delta f)$ , is defined as:

$$B_{coh} = \frac{1}{2} \left[ \arg \max_{\Delta f > 0} \left( \frac{R_H(0, \Delta f)}{R_H(0, 0)} = 0.5 \right) - \arg \min_{\Delta f < 0} \left( \frac{R_H(0, \Delta f)}{R_H(0, 0)} = 0.5 \right) \right]$$

Previous definition is essentially the -3 dB bandwidth of the correlation function.

There is also an inequality relationship to define the coherence bandwidth using the RMS delay spread  $S_T$  parameter, defined as follows:

$$B_{coh} \geq \sim \frac{1}{2\pi S_T}$$

This relation is obviously related to the fact that the  $S_T$  is derived from the Power Delay Profile  $P_h(\tau)$  while  $B_{coh}$  is obtained from the frequency correlation function, which is the Fourier transform of the Power Delay Profile.

Analogously, the definition of the coherence time  $T_{coh}$  is thus analogous to the coherence bandwidth. In this case, the coherence time is obtained from the temporal correlation function, which is a measure of how fast a channel changes. Obviously, the  $T_{coh}$  also has an uncertainly relationship with the RMS Doppler spread.

Next figure summarizes the relationships between system functions, correlation functions, and special parameters.

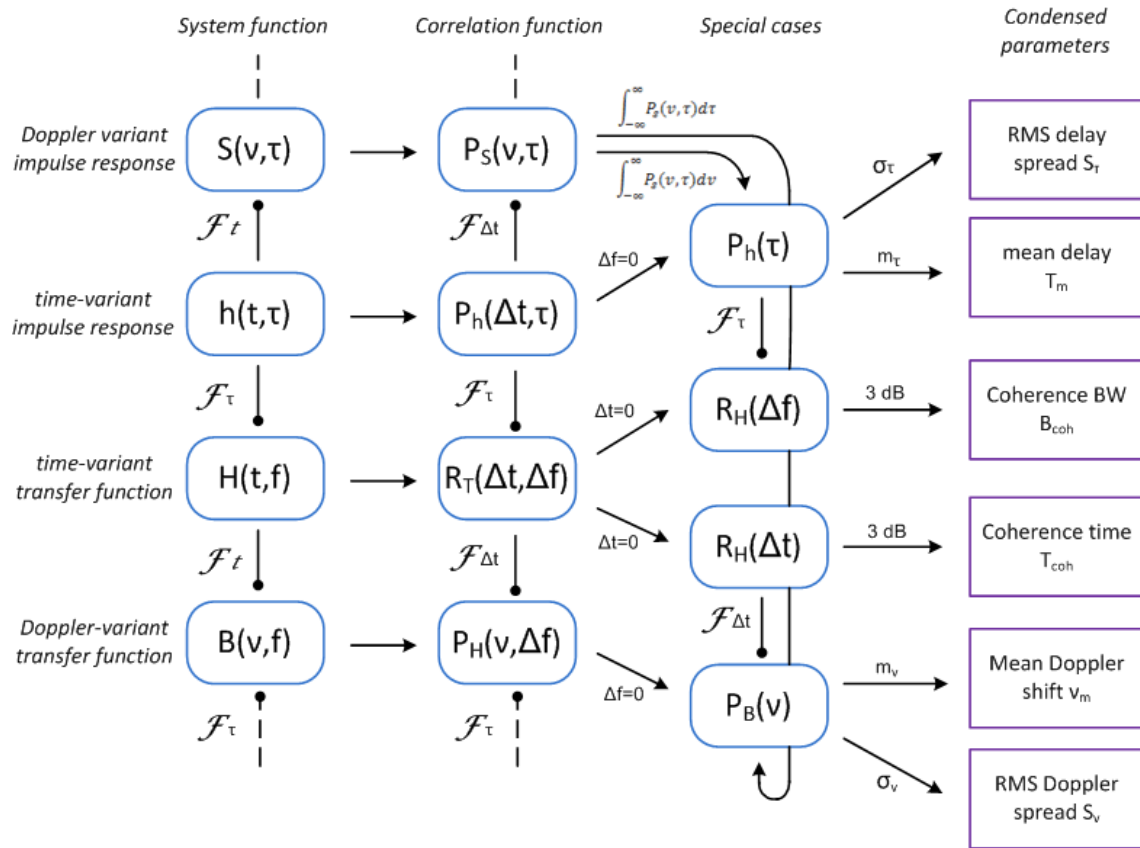


Figure 5. Summary of system functions, correlation functions, and special parameters

## 2. Technologies and Physical Layer Modes

Prior to carry on a channel estimation of the current project based on IEEE Std 802.15.3c-2009 [1] specifications it is necessary to define the working scenario. Previous chapter describe all the basis of the medium where the communication process will be performed, the wideband radio channel; however it is also important to know the working principle of the above specifications to achieve successful channel estimation. This chapter is devoted to explain the different technologies applied in such a project as well as to define the physical layer modes and structures that will be used for channel estimation based on IEEE Std 802.15.3c-2009.

### 2.1. Technologies

Taking into account the gathered specifications in IEEE Std 802.15.3c-2009 [1], there are three different physical layer (PHY) modes that have to be considered: Single carrier (SC), High-speed interface (HSI) and Audio/video (AV) mode.

These three modes will operate using two different transmission techniques. For the first one, it will be used single carrier (SC) to transmit all the data between transmitter and receiver, while second and third mode will make use of orthogonal frequency division multiplexing (OFDM) technology.

Both transmissions techniques are usually implemented for the millimeter-wave wireless personal area network (WPAN) operating at 60-GHz, which manages high data rates. Then, it is very important to understand the basis of each transmission technique prior to the channel estimation in order to know how to do it in the most efficiency way.

The following sections define the work principle of Single Carrier and OFDM technology.

#### 2.1.1. Single Carrier (SC)

Single Carrier modulation uses a single carrier frequency to transmit all data symbols sequentially. In this kind of modulation, multipath dispersion in the radio channel can produce ISI causing echoes from a particular data symbol to interfere with adjacent symbols. If the level of interference is sufficient to noticeably deteriorate the radio link, then an equalizer is used at the receiver to remove the effects of ISI [2].

### 2.1.2. Orthogonal Frequency Division Multiplexing (OFDM)

Orthogonal frequency-division multiplexing (OFDM) is a type of multicarrier modulation scheme that is especially suited for high-data-rate transmission in delay-dispersive environments [3]. OFDM uses overlapped orthogonal signals to divide a frequency-selective wideband channel into a number of narrowband flat-fading channels. A block of symbols is encoded using the Fast Fourier Transform (FFT), and transmitted in parallel over a number of sub-channels, using multiple sub-carriers. Figure 6 shows OFDM principle in the frequency domain.

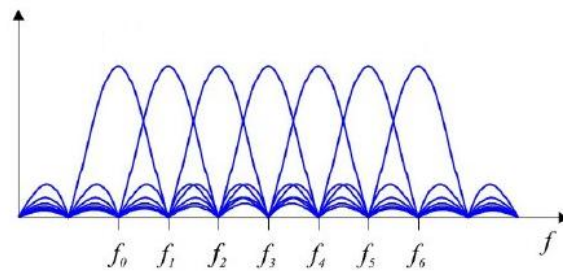


Figure 6. OFDM principle

The spectrum of each modulated sub-carrier has a sinc(x) shape since the pulses have a rectangular shape in the time domain. As can be seen, the spectra of different modulated sub-carriers overlap each other; however every carrier is in the spectral null of all the other ones. The sub-carrier frequencies are spaced apart by the inverse of the symbol time, so making them orthogonal. For  $n$  subcarriers, the symbol rate on each sub-carrier is reduced to  $1/n$  of the symbol rate for SC modulation. This ensures that the symbol period is longer than the multipath delay spread, and so reduces ISI. Some equalization is still required to correct the gain and phase of each sub-carrier.

Next Figure 7, represents the typical transceiver structure for a OFDM system. As said before, first the original data source is split into  $N$  data blocks symbols (S/P conversion) with a lower data rate. Next, each of the  $N$  data blocks are subjected to an Inverse Fast Fourier Transform (IFFT) for a time-domain conversion (Note that the input of the IFFT has  $N$  samples corresponding to the different sub-carriers, as well as its output). Afterwards, a P/S (parallel to serial) conversion is needed in order to transmit the  $N$  data values as temporal samples one after the other. Then, at the receiver, the process is repeated in the other way: sampling of the received signal, S/P conversion and perform a Fast Fourier Transform (FFT) to the data for a frequency domain conversion.

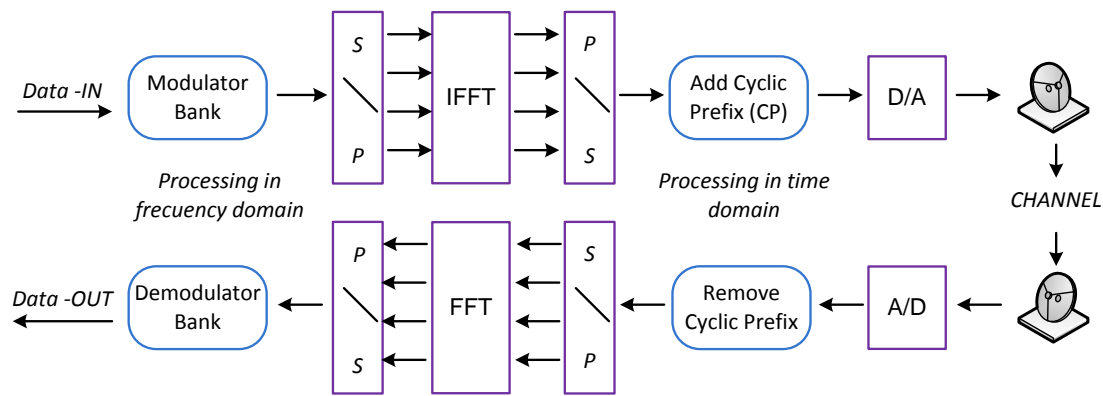


Figure 7. OFDM transceiver

The previous scheme explains the basis of how OFDM works on an Additive White Gaussian Noise (AWGN) channel. However, delay dispersion in frequency-selective channels could lead to appreciable errors such as loss of orthogonality and thus to Inter Carrier Interference (ICI); that is why a guard interval called Cyclic Prefix (CP) is introduced in order to eliminate these kind of errors.

The CP guard interval is a cyclic extension of the symbol, which in simplistic terms is a section of the start of the symbol added to the end of the symbol. Obviously, the CP has to be at least equal to the maximum excess delay of the channel in order to become effective.

The benefits of CP are two: First, as a guard interval, it eliminates ISI from the previous symbol; and second, as a repetition of the end of the symbol, it allows the linear convolution of the arriving signal (transmitted signal and channel impulse response convolution) to be modeled as a cyclical one, making easier a frequency domain processing, such as channel estimation and equalization.

It should be mention that although the concept of CP is traditionally associated with OFDM systems nowadays CP is also being used in single carrier systems to improve the robustness to multipath fading channels [5]. In fact, as it will be explained later, to make frequency-domain channel estimation over single carrier its needed a CP, allowing an easier transceiver implementation for both technologies (OFDM and SC) as well as a less different channel estimation an equalization between them.

## 2.2. Physical Layer Modes for Channel Estimation

As have been introduced before, according to the IEEE Standard, there are three different physical layer modes:

- **Single carrier (SC)** mode optimized for low power and low complexity.
- **High-speed interface (HSI)** mode optimized for low-latency bidirectional data transfer.
- **Audio/video (AV)** mode optimized for the delivery of uncompressed, high-definition video and audio.

In the following sections, PHY modes will be described focusing mainly in those parts that will be required for the channel estimation, such as data-frame structures, channel estimation sequences, pilots, Golay sequences, among others.

### 2.2.1. Single carrier (SC)

For the Single Carrier mode the PHY frame structure should be as shown in Figure 8.

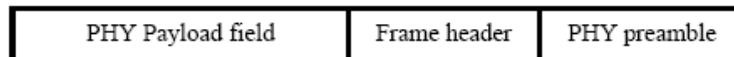


Figure 8. SC PHY frame structure

The PHY preamble contains all the information required for channel estimation as it will be explained later. The Frame Header field shall be formatted as illustrated in Figure 9 and it has important headers for communication like the MAC header and subheader. The PHY Payload field consists of the MAC frame body, stuff bits and the PCES, being this one an optional header used for channel estimation if required as it will be described later.

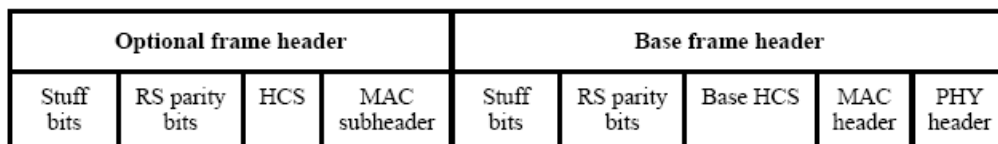


Figure 9. SC Frame Header structure

The frame will be transmitted using the following sequence: First, the PHY preamble is sent, followed by the base frame header and the optional frame header, and finally followed by the PHY Payload field.

## PHY preamble

The PHY preamble is added before the frame header to aid receiver algorithms related to AGC setting, antenna diversity selection, timing acquisition, frequency offset estimation, frame synchronization, and channel estimation.

Figure 10 shows the structure of the PHY preamble.

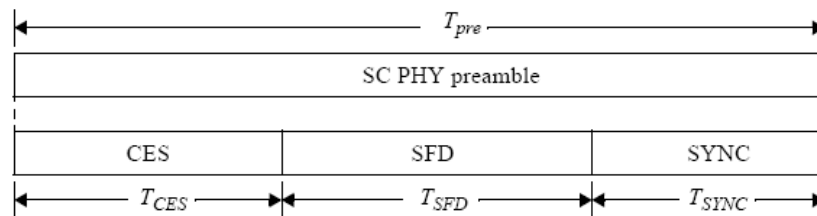


Figure 10. SC PHY Preamble structure

### Frame synchronization (SYNC)

The SYNC field is used for frame detection and it has a code repetition for higher robustness.

It should be mention that the code repetitions are based on Golay sequences, which are hexadecimal sequences with a particular pattern that will be analyzed in next chapters. This kind of sequences will be used in many headers.

For the SYNC field, it will consist of 14 code repetitions of **a**<sub>128</sub> Golay sequence, whose pattern is being defined in next figure 11.

Sequence name	Sequence value
<b>a</b> <sub>128</sub>	0x0536635005C963AFFAC99CAF05C963AF
<b>b</b> <sub>128</sub>	0x0A396C5F0AC66CA0F5C693A00AC66CA0

Figure 11. Sequence value for Golay Sequence **a**<sub>128</sub> and **b**<sub>128</sub>

### Start frame delimiter (SFD)

The SFD is used to establish frame timing as well as the header rate, either medium rate or high rate. Depending on the rate, The SFD for the two headers will be different:

- The medium rate header shall use a SFD with [+1 -1 +1 -1] spread by **a**<sub>128</sub>.
- The high rate header shall use a SFD with [+1 +1 -1 -1] spread by **a**<sub>128</sub>.

### Channel estimation sequence (CES)

The CES field is the most important header that will be used in this project. CES field contains all the necessary data that will be required for channel estimation. It consists of a frame formed by the following Golay sequences:  $[b_{128} \ b_{256} \ a_{256} \ b_{256} \ a_{256}]$  where the  $a_{256}$  sequence will be the first one in transmission.

The Golay complimentary sequences of length 128, denoted by  $a_{128}$  and  $b_{128}$ , are shown in previous figure 11. The Golay sequences of length 256, named  $a_{256}$  and  $b_{256}$ , are defined as:

$$a_{256} = [a_{128} \ b_{128}]$$

$$b_{256} = [a_{128} \ \overline{b_{128}}]$$

Being  $b_{128}$  and  $\overline{b_{128}}$  the first one to transmit for each sequence, and  $\overline{b_{128}}$  the binary-complement of the sequence  $b_{128}$ , denoted by an overline on it.

### PHY payload

#### Subblocks and pilot word

Pilot words are used in SC PHY for timing tracking, compensation for clock drift and compensation for frequency offset error. Furthermore, pilot words are also used as a known cyclic prefix and enables frequency domain equalization. In frequency domain equalization, the data is handled in the unit of subblocks, which normally corresponds to a data length equally to the sequence length used for equalization (in this case Golay sequence length of 256) plus the pilot word. The building of the data blocks and subblocks is illustrated in Figure 12.

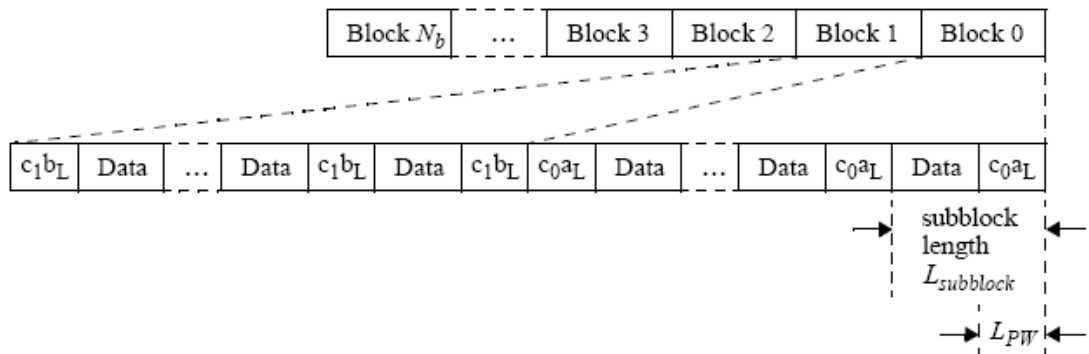


Figure 12. Pilot Word structure using data blocks and subblocks

Each block shall contain 64 subblocks with the exception of the last block (i.e., the  $N_b$ -th block). As said before, a subblock is formed by appending a pilot word to the data. The possible



pilot word lengths are 0, 8 and 64. For pilot word lengths 0 and 64, the length of the data is  $L_{DC} = L_{subblock} - L_{PW}$  symbols. For  $L_{PW} = 8$ , every subblock consists of 8 sub-subblocks each with  $L_{PW} = 8$  and  $L_{DC} = L_{subblock} / 8 - L_{PW}$ , thus giving the effective length of pilot word and data that is equivalent to that with  $L_{PW} = 64$ .

The Golay sequences for pilot word length 8 are given in Figure 13 while for pilot word of length 64 are shown in Figure 14.

Sequence name	Sequence value
<b>a<sub>8</sub></b>	0xEB
<b>b<sub>8</sub></b>	0xD8

Figure 13. Sequence value for Golay Sequence a<sub>8</sub> and b<sub>8</sub>

Sequence name	Sequence value
<b>a<sub>64</sub></b>	63AF05C963500536
<b>b<sub>64</sub></b>	6CA00AC66C5F0A39

Figure 14. Sequence value for Golay Sequence a<sub>64</sub> and b<sub>64</sub>

Another consideration is that even number blocks shall use pilot word sequences of type **a** while odd number blocks shall use pilot word sequences of type **b**. Furthermore, an LFSR (linear feedback shift register) shall be used to change the polarity of pilot word from one block to another. The last subblock of the block shall be followed by a pilot word as well.

### ***PCES***

To begin with, channel estimation will be carry on by using just the CES field. Nevertheless, there is another important field that could be useful in case the CES channel estimation is not enough to ensure a correct equalization. Pilot channel estimation sequence (PCES) insertion is an optional feature that allows the device to periodically re-acquire the channel. To add the PCES, the MAC frame body is divided into data blocks. Each data block, is divided as shown in Figure 12, and shall be preceded by a PCES, with the exception of the first block.

The PCES field shall have the same pattern as the CES field in the preamble, defined previously.

### 2.2.2 High-speed interface (HSI)

The HSI PHY frame has the same parts as the SC PHY frame. Thus, it should be formed as illustrated in Figure 15.



Figure 15. HSI PHY frame structure

The same happens to the Frame Header field for the HSI PHY frame. It shall be as shown in Figure 16.

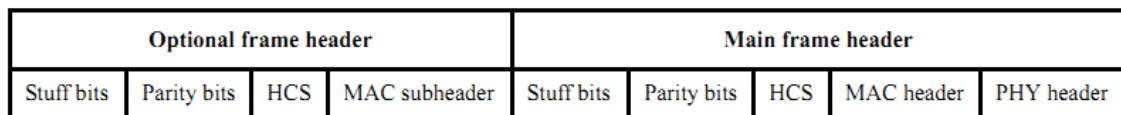


Figure 16. HSI Frame Header structure

The goal of this frame header is to convey necessary information about both the PHY and the MAC to aid decoding of the PHY Payload at the receiver.

The PHY Payload field is formed by adding any necessary stuff bits to the MAC Frame Body field, to align the data stream on the boundary of an OFDM symbol. Furthermore, the optional PCES may be added to the PHY Payload field too.

#### PHY preamble

A PHY preamble is added prior to the frame header to provide the receiver algorithms related to AGC setting, timing acquisition, frequency offset estimation, frame synchronization, and channel estimation.

The PHY preamble shall be transmitted at the rate equal to the subcarrier frequency spacing. A preamble symbol is defined as a sequence of length 512 chips that corresponds to the FFT length.

There are two preambles defined for the HSI PHY mode: the long preamble and the short preamble. The type of preamble that shall be used in the next frame can be selected by using the Preamble Type field in the PHY header. The short preamble has the same structure as defined for the SC PHY mode, and also the SYNC, SFD and CES remains the same. The long preamble has the same structure as defined for the Common Mode Signal (CMS), which is a low data rate SC PHY mode specified to enable interoperability among different PHY modes.

Thus, the CMS preamble, or the long version of the HSI PHY preamble, has the following parts:

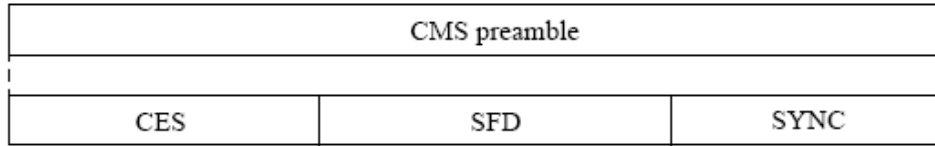


Figure 17. HSI PHY Preamble structure

The SYNC field is used primarily for frame detection and shall consist of 48 repetitions of **b128**.

The SFD field is used to establish frame timing and shall have the following scheme [+1 -1 +1 +1 -1 -1 -1] spread by **b128**.

The CES field is used for channel estimation and shall consist of **b128 b256 a256 b256 a256 a128** with **a128** first in time.

Note that, all the Golay sequences pattern have been introduced before in the SC PHY section.

### PHY payload

#### ***PCES***

The optional pilot channel estimation sequence (PCES) symbols are used for channel re-acquisition or tracking. Its content is identical to that of the CES of the short preamble type preceded by **a128**.

If PCES is used then the PCES symbols shall be inserted periodically in the PHY payload field as shown in Figure 17 The value, by specifications, of the exact period  $N_{PCES}$  shall be 96 OFDM symbols.

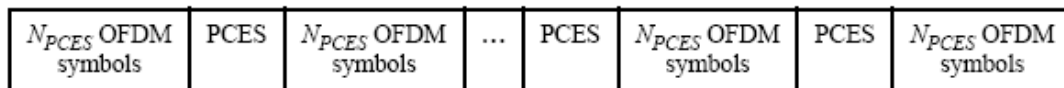


Figure 18. PCES positions in the PHY Payload field

### 2.2.3 Audio/Video (AV)

This physical layer model has two different kinds of protocols depending on the transmission.

### 2.2.3.1. High Rate Protocol Data Unit

The high rate protocol data unit (HRPDU) shall be used only in directed Channel Time Allocations (CTAs) and not in CPs, broadcast CTAs or multicast CTAs. This protocol shall be formatted as illustrated in next figure.

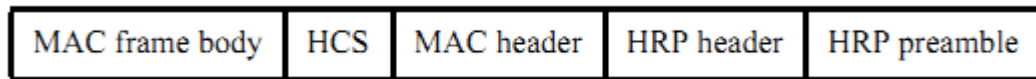


Figure 19. AV HRPDU structure

More details about the HRP preamble assembly are available in section 12.4.3.1 of the IEEE Std 802.15.3c-2009 [1].

### 2.2.3.2. Low Rate Protocol Data Unit

Two types of low-rate protocol data units (LRPDUs) are defined based on the transmitter antenna setting: *omni LRPDU* and *directional LRPDU*. Omni LRPDU are used for broadcast/multicast LRP frames, such as beacons and frames sent during contention periods, and may also be used for sending MAC commands and data. The directional LRPDU, with and without payload, shall be used to acknowledge HRP frames.

The first omni LRP frame in a CTA shall be sent using the short omni LRP preamble. Subsequent LRP frames sent in a CTA shall use the long omni LRP preamble. All omni ACK frames use the short preamble and shall be used for frames sent in a CP. The beacon frame will use the long omni LRP preamble.

The omni LRPDU is defined as illustrated in Figure 20.

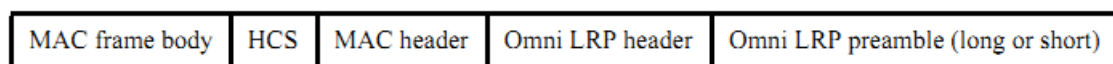


Figure 20. AV omni LRPDU structure

And the directional LRPDU is defined as follows:

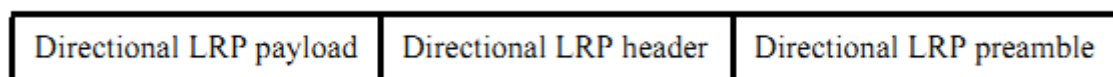


Figure 21. AV directional LRPDU structure

The long omni LRP preamble is used for frequency synchronization and blind timing recovery. It also allows devices receiving the beacon to adjust their transmit frequencies and symbol rates to the defined accuracy.

Next Figure 22 shows the long LRP preamble composition:

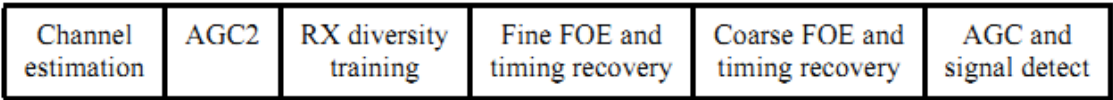


Figure 22. AV Long omni LRP preamble format

The Channel Estimation field, which is the interesting part for this project, consists of 32 blocks of 156-sample OFDM training symbols, where each block is equal to the IFFT of the 128-frequency tone vector defined in the standard, and preceded by a 28-sample cyclic prefix.

However, the short omni LRP preamble is used for limited timing adjustment and shall be configured as Figure 23.

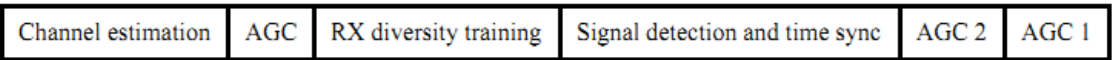


Figure 23. AV Short omni LRP preamble format

In this case, the Channel estimation field is exactly the same as the Channel estimation field for long Omni LRP preambles.

More information about this type of physical layer model can be found in section 12.4.3 of the IEEE Std 802.15.3c-2009.

### 3. Channel estimation and equalization

As have been already explained, wireless communications are affected by several phenomenon such as fading or delay dispersion due to multipath propagation, and these can lead to other effects like Inter Symbol Interference (ISI) which can disturb greatly the transmitted signal.

Thus, to minimize the fading effects the signal source is usually protected by channel coding and interleaved, and to reduce or even eliminate ISI equalizers are introduced in the receiver structures in order to improve the quality of the signal.

The claim of an equalizer is to reverse the distortions produced by the channel, to make it easy; delay dispersion corresponds to frequency selectivity when talking in the frequency domain and this to ISI effect due to a not constant transfer function over the analyzed bandwidth, thus equalizers are used to multiply the transfer function of the channel in order to obtain a constant value. Mathematically it can be expressed in the following way:

$$H(f) E(f) = \text{const}$$

Where  $H(f)$  is the transfer function of the channel and  $E(f)$  the equalizer transfer function.

And this leads also to the following “ideal” equation:

$$E(f) = \frac{1}{H(f)}$$

Where  $E(f)$  should be exactly the inverse of the channel transfer function  $H(f)$  to obtain a flat response. In fact, this is the mathematical expression used by one of the equalizers structures. However, due to the inversion of  $H(f)$ , infinity gains are produced when  $H(f)$  values are close to 0, preventing the desired constant output.

In the following sections will be introduced the most important equalizers types, classified into data-aided (which make use of a training sequence) and blind equalizers (avoiding training sequences). This will be useful to select those methods that may have better performance on simulation, not only for this project scope, but also for the next project stages depending on each criterion, also taking into account the standard IEEE Std 802.15.3c-2009 specifications. Next, it will be discussed the channel estimation algorithms that could be deployed for this and future project stages, in order to obtain the transfer function of the channel and conclude which simulated equalization would denote better performance.

### 3.1. Data-Aided Equalizers

The most common equalization works in two stages: a training phase and a detection phase. During the training phase, a known bit sequence (training sequence) is transmitted over the channel, and the received distorted sequence is compared with the original transmitted one to obtain the channel impulse response used for later equalization.

Using the training sequence also resolves the time variance phenomenon of the channel by repeating the transmission of the training sequence at intervals so that the equalizer could be adapted to the different channel states. This is known as “adaptive equalization”

But channel estimation by using data-aided structure has also the following drawbacks:

- *Reduction of spectral efficiency*, due to the fact that the training sequence does not have any useful payload information.
- *Sensitivity to noise*: in order to restrict more or less the previous problem, training sequences are short, but this also implies that the training sequence is much more sensitive to noise and thus to errors in channel estimation.
- *Outdated estimates*: this problem arises when the channel properties change after the transmission of the training sequences, then the receiver cannot detect this change and will produce decision errors.

In spite of the drawbacks, data-aided equalizers are the most commonly used because blind techniques, which will be introduced later, have high computational and numerical problems that may involve a major problem. In addition, it should be taking into account that IEEE Std 802.15.3c uses a special kind of training sequences (Golay Sequences) for channel estimation and equalization depending on the selected physical layer mode. Both reasons have been decisive in order to select Data-Aided Equalizers for Single Carrier simulations, that will be carry out in this project.

Next, it will be introduced some of the most important data aided equalizers structures, divided into linear, decision feedback equalizers and maximum-likelihood sequence estimators

#### 3.1.1. Linear Equalizers

They are simple linear filters structures whose goal is to reverse the channel, trying to obtain a product between channel and equalizer transfer functions that fulfils a determined criterion.

Depending on the criterion, it could be a Zero-forcing equalizer if the goal is to achieve a completely flat transfer function in frequency domain or Minimum Mean Square Error (MMSE) equalizer if the claim is to reduce this rate as much as possible at the filter output.

### 3.1.1.1. Zero Forcing

Zero-Forcing is the most basic equalizer structure and its coefficients try to enforce a constant transfer function in frequency domain once applied to the channel. If a transmit sequence ( $C_i$ ) is sent through the channel, a sequence ( $U_i$ ) will be received at the equalizer input, then the equalizer coefficients ( $e_n$ ) should transform the  $U_i$  sequence into  $\tilde{C}_i$  as in the following equation:

$$\tilde{C}_i = \sum_{n=-K}^k e_n U_{i-n}$$

Note that  $\tilde{C}_i$  should be as similar to  $C_i$  as possible. In fact, defining the deviation  $\varepsilon_i$  as:

$$\varepsilon_i = C_i - \tilde{C}_i$$

the aim of the Zero-Forcing equalizer is to find a filter whose coefficients follow:

$$\varepsilon_i = 0 \text{ for } N_o=0$$

being  $N_o$  the noise variance of the channel.

This method will be used in simulations in order to obtain the results for the simplest structure of equalization and compare with other equalization structures. More details about previous channel estimation, which is the basis of this equalization, and simulations results, will be shown in chapter 4 and 5 respectively.

In this way, the Zero-Forcing equalizer is ideal for elimination of ISI. Nevertheless, this kind of equalization produce noise enhancement in the spectral nulls (deep fading) due to the form of the transfer function of the equalizer, which is  $E(f) = 1/H(f)$ . Attending the previous equation, it can be deduce that the equalizer amplifies strongly (infinity gain) those frequencies with a small value of the channel transfer function, enhancing the noise too. For this reason, Minimum Mean Square Error equalizers are introduced with a different aim and pattern.

### 3.1.1.2. Minimum Mean Square Error

In general, the MMSE equalization is more efficient than Zero-Forcing, as it makes a trade-off between residual ISI (in the form of gain and phase mismatches) and noise enhancement. This is particularly attractive for channels with spectra nulls or deep amplitude depressions.



In this case the aim of the equalizer, talking in terms of deviation  $\varepsilon_i$  is:

$$E\{|\varepsilon_i|^2\} \rightarrow \min \quad \text{for } N_o \text{ with a finite value}$$

This condition tries to minimize the bit error probability instead of ISI, taking into account the Noise factor.

Thus, The MMSE transfer function will be as follow:

$$E(f) = \frac{H(f)^*}{|H(f)|^2 + 1/\eta}$$

Where  $\eta$  refers to the Signal-to-Noise ratio (SNR) and  $*$  to the conjugate transpose.

This equalization method would be also analyzed in the current simulations due to its different approach regarding ZF. More details are provided in section 4.

### 3.1.2. Decision Feedback equalizers

A decision feedback equalizer (DFE) is a nonlinear equalizer that uses channel impulse response, as well as previous detector decision, to eliminate the ISI of future samples. In other words, the ISI effect produced by this bit in subsequent samples is calculated and then subtracted from these future samples.

DFE is composed by a forward filter with transfer function  $E(f)$  and a feedback filter  $D(f)$  that can each be a linear filter structure as can be seen in Figure 24.

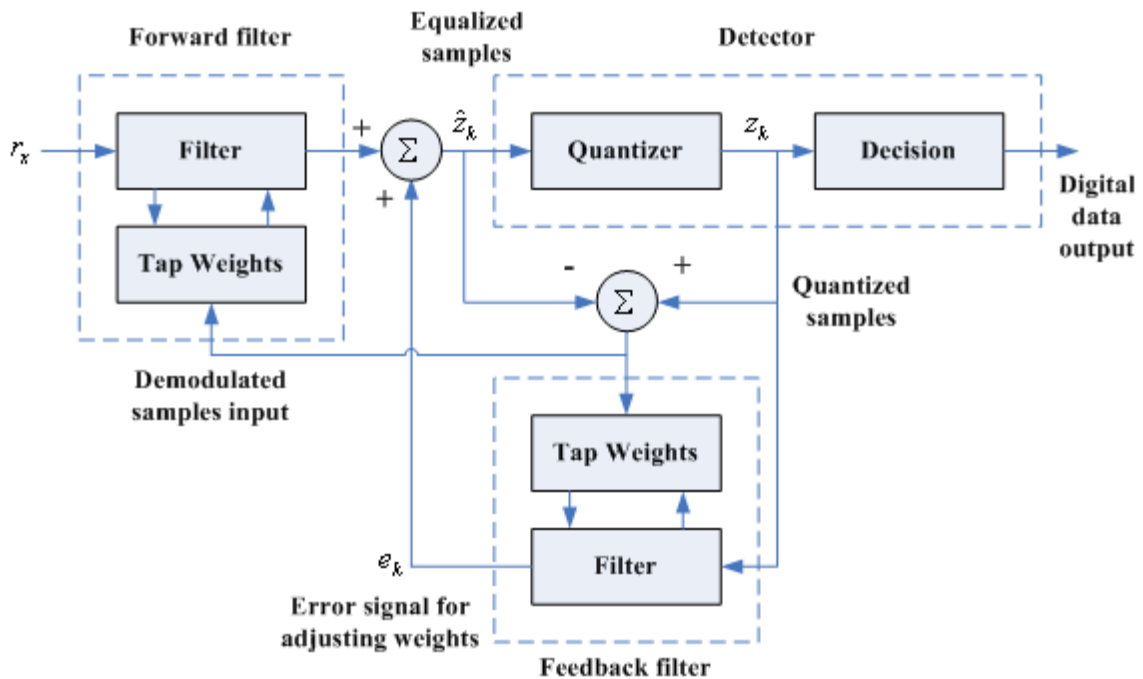


Figure 24. Decision Feedback Equalizer

The nonlinearity of the DFE stems from the nonlinear characteristic of the detector that provides an input to the feedback filter. The basic idea of a DFE is that if the values of the symbols previously detected are known, then ISI contributed by these symbols can be cancelled out exactly via the feedback filter by subtracting past symbol values with appropriate weighting. The forward and feedback coefficients weights can be adjusted simultaneously to fulfil a criterion such as Zero-Forcing or MMSE.

The advantage of a DFE implementation is the feedback filter, which is additionally working to remove ISI, and thus eliminates additive noise from the feedback signal. Then, a DFE has smaller error probability than linear equalizers.

The main drawback of this equalizer is error propagation. If the receiver takes a wrong decision for one bit, then the later computed ISI will be erroneous too, and the future samples arriving to the receiver will be even more afflicted by ISI than unequalized ones.

In this stage of the project, there is no intention to use this type of equalizers because it has a more complex structure and there is not enough time to develop it.

### **3.1.3. Maximum-likelihood sequence estimator**

The Maximum-likelihood sequence estimator (MLSE) tries to determine the sequence of symbols that has most probably been transmitted instead of focusing only in a symbol.

Its working principle is similar to decoding convolutional codes. There are various algorithms to determine the optimum sequence but the most used is Viterbi algorithm. First, the receiver generates all possible sequences that can be generated from convolution channel impulse response and valid transmitted sequences. Next, it tries to find which of the generated sequences has the best metric, in other words, which has the smallest distance from the received signal.

It should be mention that MLSE only works properly if considered white additive noise at the input of the equalizer. Then, the samples values used have to be those of the output of a noise-whitening filter, and this filter should be adapted to the current channel state.

The best advantage of MLSE is that minimization of BER (Bit-Error-Rate) is superior to that of all other structures, however the main drawback is that the computation effort increases exponentially with length of the impulse response of the channel. In fact, MLSE is the Data-Aided method with the highest power consumption and cost due to computational reasons.

For this reason, in a first step of the project, MLSE is not going to be developed for simulations. Nevertheless MLSE use is not rule out for future project stages.

### 3.2. Blind equalizers

All previous equalizers are based on channel estimation using a training sequence, a sequence of known bits, which allows the receiver to estimate the channel impulse response. Blind equalization is quite different because there is no training sequence for channel estimation. In contrast, blind equalizers take advantage of statistical properties of the signal for channel and data estimation processes, and the equalizer coefficients are adjusted in that way.

Some signal properties that can be used for blind equalization are: constant envelope of the transmitted signal, statistical properties as cyclostationary, finite symbol alphabet, and spectral correlation among others.

The advantages of blind equalization are, on the one hand that all the timeslot is used for calculation of the channel impulse response instead of just the training sequence timeslot, and on the other hand this increases also the spectral efficiency of the channel because there is no training sequence to send and this time will be used for true data transmission. Nevertheless, blind equalizers have some drawbacks that made them not suitable to replace data-aided equalizers structures. The main inconvenient is its computational effort and reliability, which requires a long time interval to converge and this is not possible in fast time-variant wireless channels. For this reason, this kind of equalization is not going to be used in this project.

Some blind equalizers algorithms are: the Constant modulus algorithm, blind MLSE estimation and second or higher order statistics algorithms .More information about them can be found in [2].

## 4. Selected Channel estimation and equalization algorithms

After the description of the different existing equalizers structures in order to reverse all distortions produced by the channel, now it will be discussed the different methods implemented in this project to achieve channel estimation and equalization.

First of all, it should be taking into account the transmission technologies operating on the project standard IEEE Std 802.15.3c, which are OFDM and Single Carrier. This is a key point because channel estimation could be made in the time or the frequency domain depending on the implemented technology to obtain better performance. As OFDM operates with a number of parallel narrowband subcarriers, it is intuitive to make frequency domain channel estimation. Taking into account Single Carrier technology, some studies have shown better performance based on frequency domain estimation than in time domain. Therefore, time-domain equalizers cannot easily handle inter symbol interference (ISI) on channels with very long impulse responses, thus frequency domain estimation will be used for both technologies achieving also compatibility between the OFDM and Single Carrier channel estimation.

Attending this consideration, Single Carrier with frequency domain equalization (FDE) is very similar to OFDM since both perform channel equalization in the frequency domain. However, their difference is the position of Inverse Fast Fourier Transform (IFFT) block operation. In OFDM, IFFT is placed in the transmitter to transform the signals from the frequency domain into time domain. In Single Carrier with FDE, IFFT is placed in the receiver, between the equalization and the data decision. Thus, the data decision is performed in time domain, whereas in OFDM, the data decision is performed in frequency domain, right after the channel equalization.

Next, in the following sections, will be defined all the necessary steps to obtain channel estimation and equalization based on two different methods: Zero Forcing and MMSE. These two methods have been selected, on the one hand because they are the most commonly used methods for equalization due to its low computational effort and easy implementation, and on the other hand because other methods used in equalization require more time and are difficult

implementations and do not offer such a great improvement in the results as could be expected.

#### 4.1. Channel estimation

Previous to equalization, channel estimation should be carried out in order to determine the channel transfer function  $H(f)$ . There are several methods to estimate  $H(f)$ , for example by using the pilot signals in OFDM or a training sequence. In this project, channel estimation will be done by using the golay sequences defined in the PHY specifications, which is the equivalent of training sequence estimation but with some differences that will be explained in the next section.

##### 4.1.1. Golay Sequences

As described in chapter 2, the channel estimation sequence preamble (CES) is based on complementary Golay sequences which consists of two different parts, “**a**” and “**b**”. The most important feature of these Golay sequences is that both parts are complementary between them, in other words, the sum auto-correlation of the pair (“**a**” and “**b**”) has a unique peak and zero sidelobe, which is effectively used to remove the inter-symbol interference (ISI) of the channel and to improve the accuracy of channel estimation.

Then, to calculate the channel frequency response  $H(f)$  the following steps should be considered.

Being  $N_{CE}$  the number of nonzero channel impulse response (CIR) taps, which depends on the length of each Golay sequence (normally 128 or 256) the delay profile of the wireless channels. The CIR vector estimated by the autocorrelation of “**a**” sequence is:

$$h_{a,g} = (h_a[g, 0], h_a[g, 1] \dots h_a[g, i] \dots h_a[g, N_{CE} - 1])$$

where  $h_a[g, i]$  is the  $i$ -th channel impulse response tap estimated by the golay sequence “**a**” in the  $g$ -th CES preamble (which is made up of  $G$  repetitions of CES).

In the same way the CIR vector estimated by the autocorrelation of “**b**” sequence is:

$$h_{b,g} = (h_b[g, 0], h_b[g, 1] \dots h_b[g, i] \dots h_b[g, N_{CE} - 1])$$

In order to better understand the golay sequences properties, the following Figure 25 and 26 from [3] shown an example of the autocorrelation for each pair of sequences “a” and “b”.

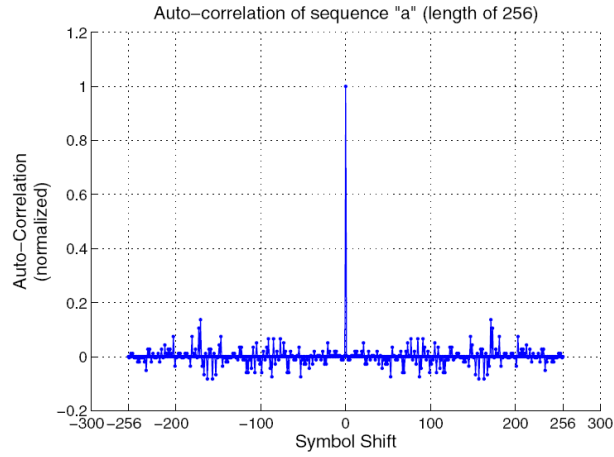


Figure 25. Autocorrelation of Golay Sequence “a”

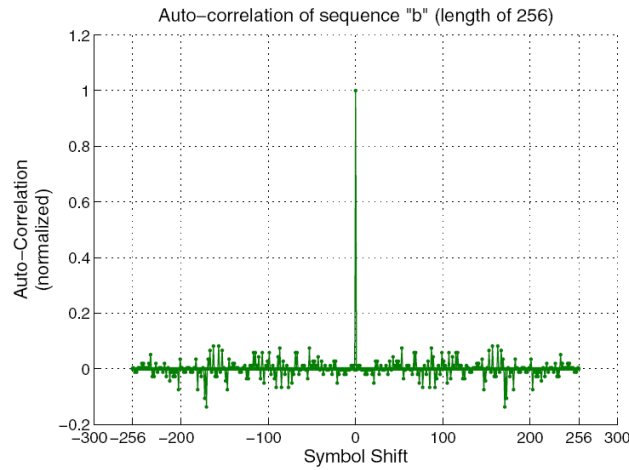


Figure 26. Autocorrelation of Golay Sequence “b”

Now, applying the sum auto-correlation property of complementary Golay sequence, we average  $h_{a,g}$  and  $h_{b,g}$  to get the CIR vector (estimated by the  $g$ -th CES) as follows:

$$h_g = \frac{h_{a,g} + h_{b,g}}{2} = (h[g, 0], h[g, 1] \dots h[g, i] \dots h[g, N_{CE} - 1])$$

And the resulting representation for the previous stated example is shown in Figure 27.

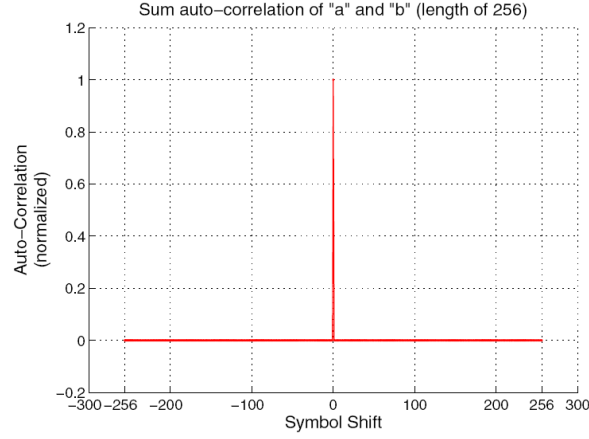


Figure 27. Sum-Autocorrelation of Golay Sequences “a” and “b”

#### 4.1.2. Channel estimation process

Before the application of the Golay sequences properties, it is required to obtain  $h_a$  and  $h_b$  sequences, which correspond to the estimated CIR, after passing through the channel, of sequences “a” and “b”.

In fact, the symbol received at the receiver  $r(t)$  is expressed as follows:

$$r(t) = \sum_{v=0}^{T_{CH}-1} h(t) s(t-v) + n(t)$$

where  $h(t)$  is the CIR including wireless channel and filters,  $T_{CH}$  is the length of CIR and  $n(t)$  is additive white Gaussian noise. It must be pointed out that, for sake of simplicity, it has been assumed that  $T_{CH} \leq N_{CE}$ , in other case the CIR estimation will be incorrect.

Obviously, previous equation it is also true for the received symbols corresponding to the CES sequence, as:

$$r_{CE}(t) = \sum_{v=0}^{T_{CH}-1} h(t) s_{CE}(t-v) + n(t)$$

Then, in order to obtain  $h_a$  and  $h_b$ , for each g-th CES repetition, it must be done the correlation between the original transmitted Golay sequences ( $a_{N_{CE}}$  and  $b_{N_{CE}}$ ) and the received  $r_{CE}(t)$ , as defined in the following equations:

$$h_{a,g}(t) = \frac{1}{N_{CE}} \sum_{d=0}^{N_{CE}-1} r_{CE}(t+d-N_{CE}+1) a_{N_{CE}}^*(d)$$

$$h_{b,g}(t) = \frac{1}{N_{CE}} \sum_{d=0}^{N_{CE}-1} r_{CE}(t+d-N_{CE}+1)b_{N_{CE}}^*(d)$$

where  $N_{CE}$  is the length of each Golay sequence and \* means the conjugate transpose of each sequence.

Next, taking benefit of Golay sequences properties, the CIR  $\hat{h}_g(t)$  corresponding to the g-th CES repetition, is estimated by sum and average operation over  $h_{a,g}(t)$  and  $h_{b,g}(t)$ , as below:

$$\hat{h}_g(t) = \frac{h_{a,g}(t) + h_{b,g}(t)}{2}$$

Or it can be obtain directly, the averaged estimated CIR  $\hat{h}(t)$  by applying previous equation over the G number of repetitions of the CES:

$$\hat{h}(t) = \frac{1}{2G} \sum_{p=0}^{G-1} h_a(t+pG) + h_b(t+pG)$$

Finally in order to perform Frequency Domain Equalization, the channel frequency response CFR  $H[k]$  is obtained from CIR  $\hat{h}(t)$  as the FFT of  $N_{CE}$  points:

$$H[k] = \sum_{i=0}^{N_{CE}-1} \hat{h}(i) e^{-j(\frac{2\pi}{N_{CE}}i)}$$

It should be taken into account that all transfer functions expressed here are time variant. Nevertheless for a simple notation the time variant parameter has not been included in the equations.

## 4.2. Zero Forcing Channel Equalization

To achieve Zero Forcing Equalization, first it should be estimated the transfer function of the channel  $H(f)$ , as described before.

Next, the coefficients of the  $k$ -th subcarrier  $C[k]$  of the Zero forcing equalizer can be determined using the following equation:

$$C[k] = \frac{1}{H[k]}$$

The result of an equalization based on the zero-forcing (ZF) criterion, which aims at canceling ISI regardless of the noise level, will be presented in section 5.



### 4.3. MMSE Channel Equalization

For the MMSE channel equalization it is also required the channel transfer function previously presented in order to determine the  $C[k]$  coefficients for this kind of equalizer.

However, as had been seen in previous section, MMSE equalization not only takes into account the transfer function of the channel, but also the SNR ( $\eta$ ) due to the aim of a different approach that considers noise variance, compared to Zero- Forcing equalization. Thus, it is necessary to estimate the SNR value as would be seen in section 4.3.1.

Once calculated the transfer function and SNR value, the MMSE coefficients can be calculated as:

$$C[k] = \frac{H[k]^*}{|H[k]|^2 + 1/\eta}$$

Being, as defined in chapter 3,  $\eta$  the Signal-to-Noise ratio (SNR) and  $H[k]^*$  the conjugate transpose of  $H[k]$ .

The simulations based on MMSE equalization, which tries to minimize the combined effect of ISI and noise, are shown in section 5.

#### 4.3.1. SNR Estimation

The Signal to Noise ratio (SNR) is a measure used to quantify how much a signal has been corrupted by noise. The higher the SNR, lower noise compared to the signal level. As had been said before, it is necessary to estimate SNR in order to obtain a correct MMSE channel equalization. SNR estimation will be calculated by applying the following steps.

The noise at the  $k$ -th subcarrier in the  $g$ -th repetition of the CES can be quantified as:

$$W[g, k] = H[g, k] - H[k]$$

Where  $H[g, k]$  correspond to the estimated CFR  $H[k]$  by the  $g$ -th repetition, defined by the following equation:

$$H[g, k] = \sum_{i=0}^{N_{CE}-1} \hat{h}_g(i) e^{-j(\frac{2\pi}{N_{CE}})}$$

The signal power can be estimated as:

$$P_s = \frac{1}{N_{CE}} \sum_{k=1}^K |H[k]|^2$$

And noise power can be estimated then as:

$$P_n = \frac{1}{GN_{CE}} \sum_{g=1}^G \sum_{k=1}^K |W[g, k]|^2$$

Thus, the estimated SNR ( $\eta$ ) is:

$$\eta = \frac{P_s}{P_n}$$

## 5. Simulations

### 5.1. Simulation System and Scenario

This section explains the development of the simulation system that will be used to test the IEEE 802.15.3c standard, not only for this project stage which is focus into channel estimation performance and simulations for Single Carrier technology, but also in next project stages where it will be analyzed other specifications such as OFDM technology. This scenario and the resulting simulations have been carried out in Matlab/Simulink being some of the used blocks directly imported from Matlab/Simulink libraries and others blocks developed from scratch.

The communication process was clearly divided in three stages: transmission part, channel simulation, and reception.

Basically, the transmission stage is made up of a bit generator which will represent the useful information (payload) of the full transmitted sequence, and a modulator bank that will convert the bit stream into symbols able to be transmitted over an analog channel or a limited radio frequency band.

For the channel simulation, pulse shaping filters have been introduced in order to reduce Intersymbol Interference. Furthermore, to simulate different channel responses over the transmission process, a digital filter has been introduced, and to represent the noise variations which will affect the transmitted signal it has been placed an Additive White Gaussian Noise (AWGN) channel.

Finally, in reception, the received signal will be demodulated in order to turn back the information to a bit stream. Next, the received and transmitted bits will be compared in order to know how many bits were successfully recognized at reception after passing through the channel, or in other words, how many bits were erroneous after transmission by means of the Bit Error Rate (BER). It will be also in this stage were the equalization will be done and results would be compared.

Next Figure 28 shows the different blocks required in Simulink for the whole communication transmission system simulator.

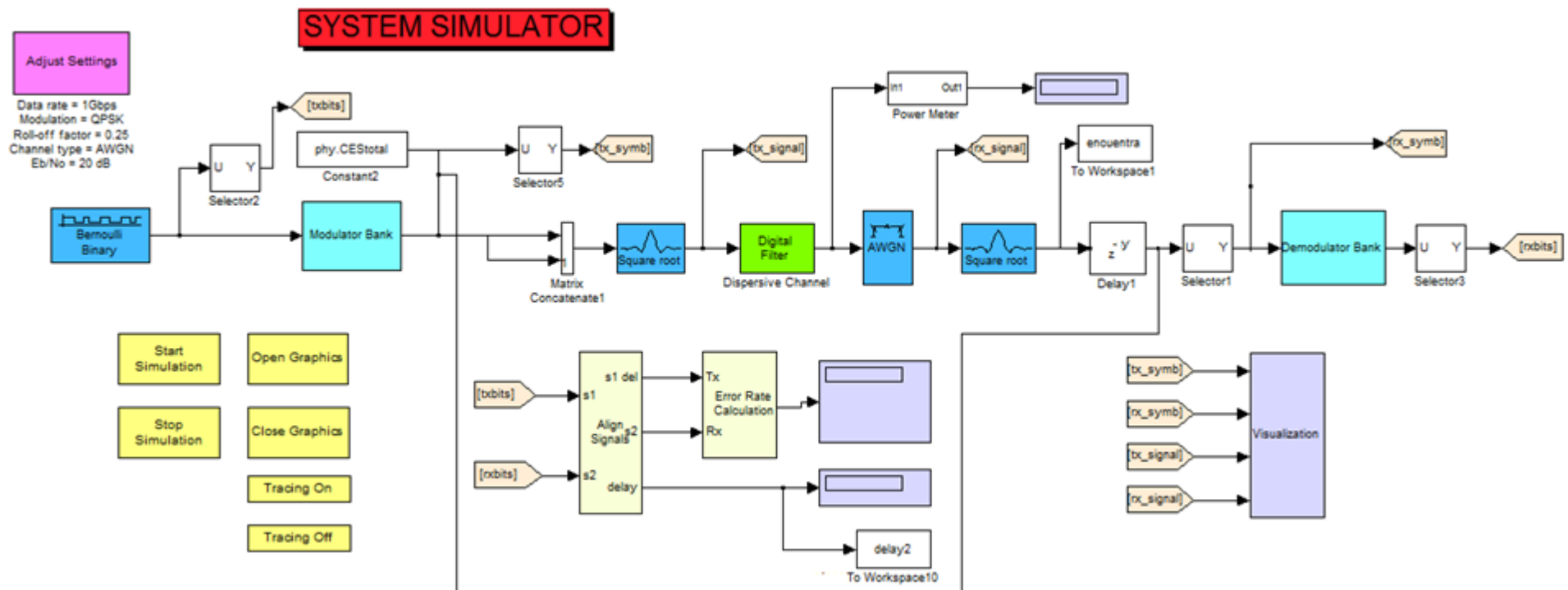


Figure 28. System Simulator

It is important to say that some general parameters will be defined previously using an initialization code in Matlab (“Adjust Settings Block” of Figure 28), however other specific characteristics will be defined directly in each block parameters. Other functions such as Golay Sequences Generation, Hexadecimal to binary transformation or graphics generation will be also developed as a Matlab code file.

In the following sections, the different elements or blocks used for simulation will be defined concretely and adapted to introduce a properly equalization, according and taking into account the specifications collected in the standard 802.15.3c.

## Modulator bank

The modulator bank, as said before, converts the bit stream into symbols able to be transmitted over an analog channel or a limited radio frequency band.

This modulator bank will be interchanged by the different modulation schemes that include the current specifications of 802.15.3c which supports BPSK, QPSK, 8-PSK and 16-QAM (it also includes DBPSK and 32 QAM modulations for other future simulations).The modulator bank has been developed as follows by taking the simple supported modulator structures from Matlab libraries or previously developed and provided by TU University.

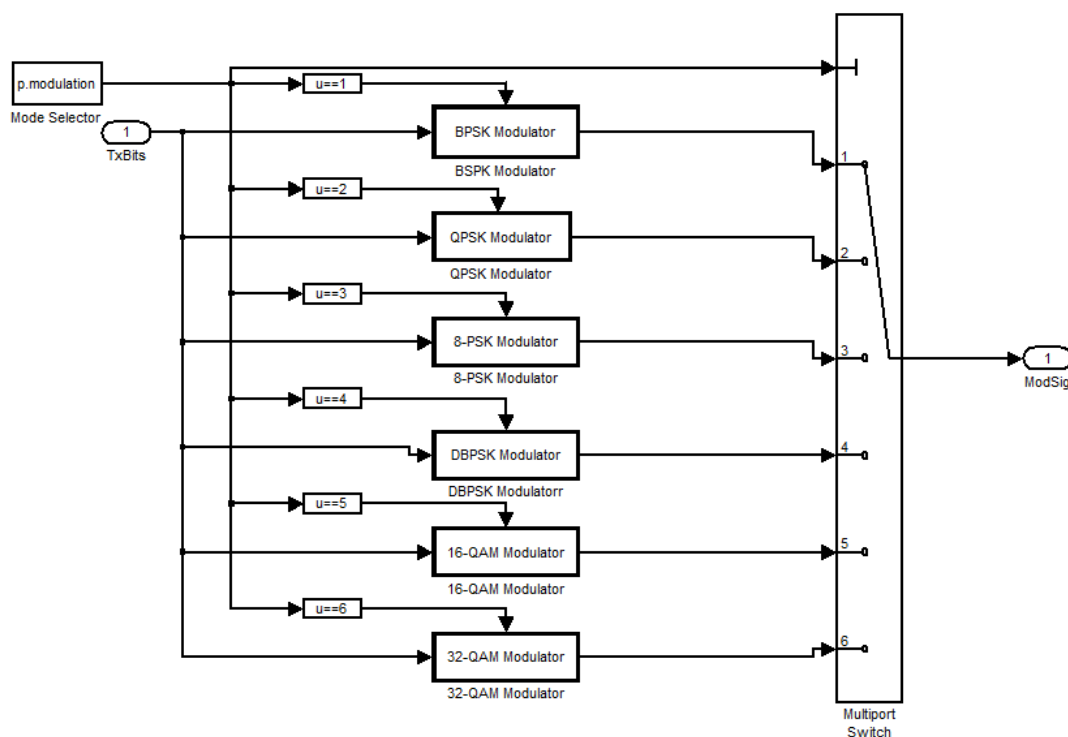


Figure 29. Modulator Bank

## Demodulator bank

The demodulator bank has almost the same structure as the modulator bank. Nevertheless his function is totally opposed to that of the modulator bank since the demodulator converts the symbols transmitted through the channel into a bit stream easily to understand for the system.

The following figure presents de demodulation structure taking into account all different modulations supported by the standard:

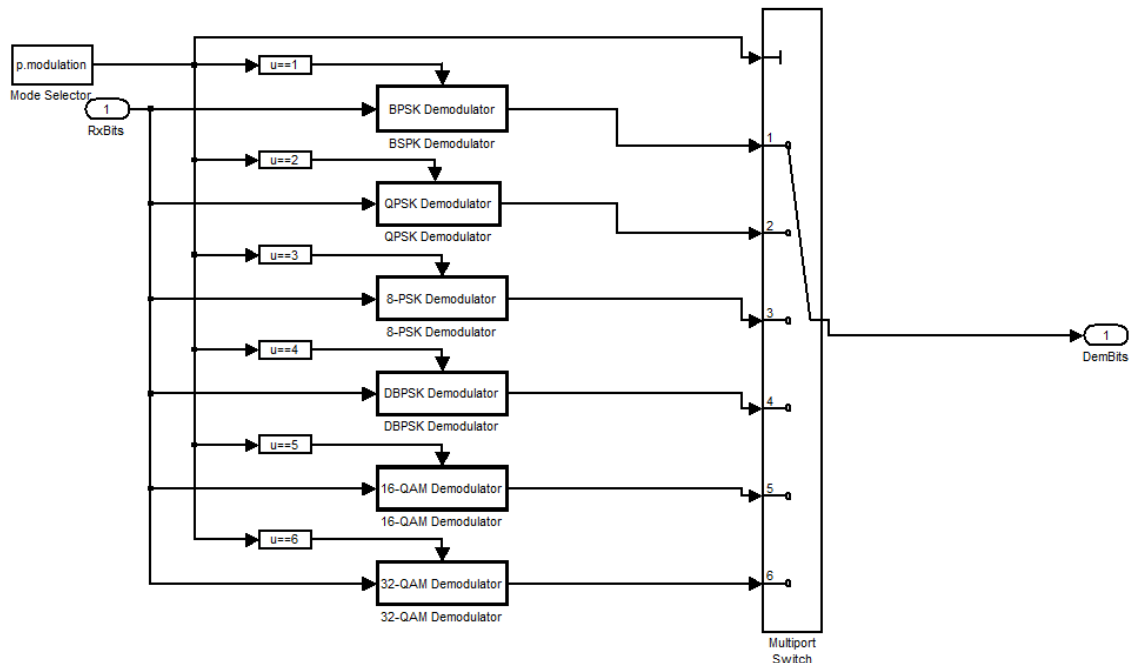


Figure 30. Demodulator Bank

## Pulse shaping filters

Transmitting a signal at high modulation rate through a band-limited channel can create intersymbol interference. As the modulation rate increases, the bandwidth of the signal increases and when it becomes larger than the channel bandwidth, the channel starts to introduce distortion to the signal, which is seen as intersymbol interference.

Usually the transmitted symbols are represented as a time sequence of dirac delta pulses. This theoretical signal is then filtered with the pulse shaping filter, producing the transmitted signal, and reducing the intersymbol interference. The spectrum of the transmission is thus determined by the filter.

This block is part of the Simulink library and it does not need to be developed; however it has the following characteristics that have to be specified:

- The **Filter type** parameter determines which type of filter the block uses; choices are Normal and Square root. For the demonstrations it will be selected the Square root type, taking into account that the impulse response of a square root raised cosine filter convolved with itself is approximately equal to the impulse response of a normal raised cosine filter. This is important because in the model it will be used two almost equal square root filters, one for upsampling the input signal and the other one to downsampling it.
- The **Upsampling & Downsampling factor** which is related to the framing method. The value of this parameter determines the characteristics of the output signal. Thus, if the input is a sample-based scalar, then the output is sample-based scalar whose time is N times the input sample time. This parameter is fixed to 8.
- The **Group delay** parameter is the number of symbol periods between the start of the filter's response and the peak of the filter's response and it will be set up to 4. The group delay and the upsampling factor, N, determine the length of the filter's impulse response, which is  $2 * N * \text{Group delay} + 1$ .
- The **Rolloff factor** parameter is the filter's rolloff factor. It must be a real number between 0 and 1. The rolloff factor determines the excess bandwidth of the filter. For example, a rolloff factor of 0.5 means that the bandwidth of the filter is 1.5 times the input sampling frequency. For the simulations it will be set up to 0.25.

In the following figure, it can be seen the change of shape of a Raised Cosine in the amplitude response with various roll-of factors  $\beta$ .

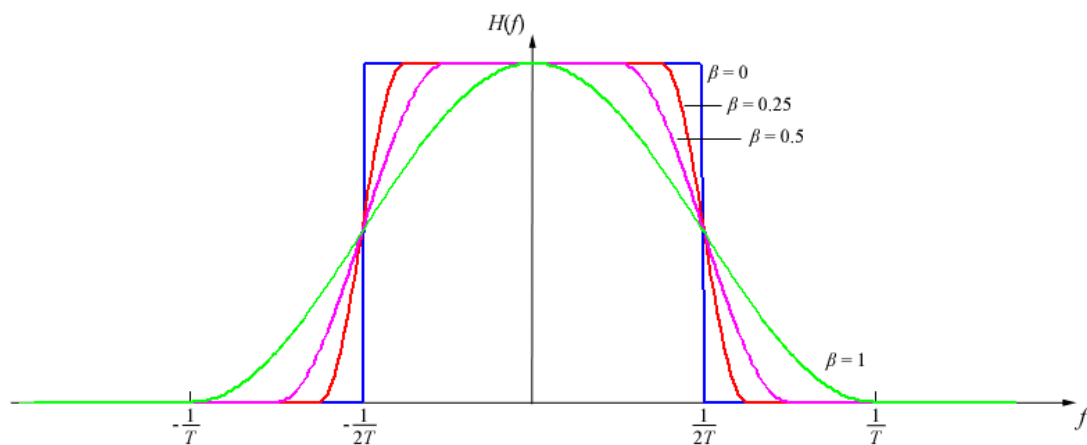


Figure 31. Amplitude response of raised Cosine with various roll-off factors

- The **Filter gain** parameter indicates how the block normalizes the filter coefficients. Selecting the Normalized option the block normalizes the filter coefficients so that the peak coefficient is equal to 1.

### Additive White Gaussian Noise (AWGN)

An AWGN channel is a model in which the only deterioration to communication transmission is a linear addition of white noise with a constant spectral density and a Gaussian distribution of amplitude.

This model does not account for fading, frequency selectivity, interference, nonlinearity or dispersion. However, it produces simple and tractable mathematical models which are useful for gaining insight into the underlying behavior of a system before these other phenomena are considered.

Wideband Gaussian noise comes from many natural sources, such as the thermal vibrations of atoms in conductors (referred to as thermal noise), shot noise, black body radiation from the earth and other warm objects, and from celestial sources such as the Sun.

Simulink already offers an AWGN block that will be used for simulations, nevertheless some parameters have to be defined in order to work. The parameters that have to be defined are:

- **Mode:** It defines the variance of the noise generated by the AWGN Channel block. There are several models such as  $E_b/N_0$ ,  $E_s/N_0$  or SNR. In order to represent the final results in the most common way, it will be selected  $E_b/N_0$  mode. It should be taken into account that  $E_b/N_0$  is the energy per bit to noise power spectral density ratio). This parameter is a normalized signal-to-noise ratio (SNR) measure, also known as the "SNR per bit" and it is especially useful when comparing the bit error rate (BER) performance of different digital modulation schemes without taking bandwidth into account.
- **Number of bits per symbol:** This will depend on the modulation used in each simulation. For example, choosing BPSK modulation will set up this value to 1 and for a QPSK modulation it will be modified to 2.
- **Input signal power:** It refers to the actual power of the symbols at the input of the block. This value is especially important because if it is not chosen properly, then noise power may not be noticeable or exceed the input signal power, being impossible to



differ between noise and input signal preventing to obtain some results. In order to obtain this value it will be used a simulated **power meter**.

- **Symbol period (s):** The duration of a channel symbol, in seconds. This parameter will depend on the signal modulation and channel bandwidth or data rate.

## Digital Filter

The Digital Filter will define the specific channel effects since the AWGN channel only introduces linear White noise. This model will take into account fading, frequency selectivity, interference, nonlinearity or dispersion of the channel depending on the channel definition that will be used to carry on the tests. This filter added to the AWGN model channel will be enough to obtain a simulation system that represents the equalization system behavior under real operating conditions, taking into account all necessary considerations defined on the project standard.

The Digital Filter block independently filters each channel of the input signal with a specified digital IIR or FIR filter. In this case it will be defined a FIR filter with a Direct-form structure because the filter coefficients that are being introduced are defined a Numerator coefficient Vector (No denominator coefficients).

In order to obtain the Numerator Coefficient Vector it has been used data provided by TU University from different propagation scenarios where the frequency response has been captured.

In order to convert this information into understandable filter coefficients for the subsequent representation of the impulse response, it has been performed the following steps:

- 1- Selection of those discrete frequency responses which are within the bandwidth range for operation defined in the Standard 802.15.3c.
- 2- Resample function of the selected data to fit a measure that is a power of 2.
- 3- Use of the Inverse Fourier Transform to obtain the channel impulse response: Numerator Coefficient Vector.

The frequency response of the channels that will be simulated in this project are shown below:

### CHANNEL A

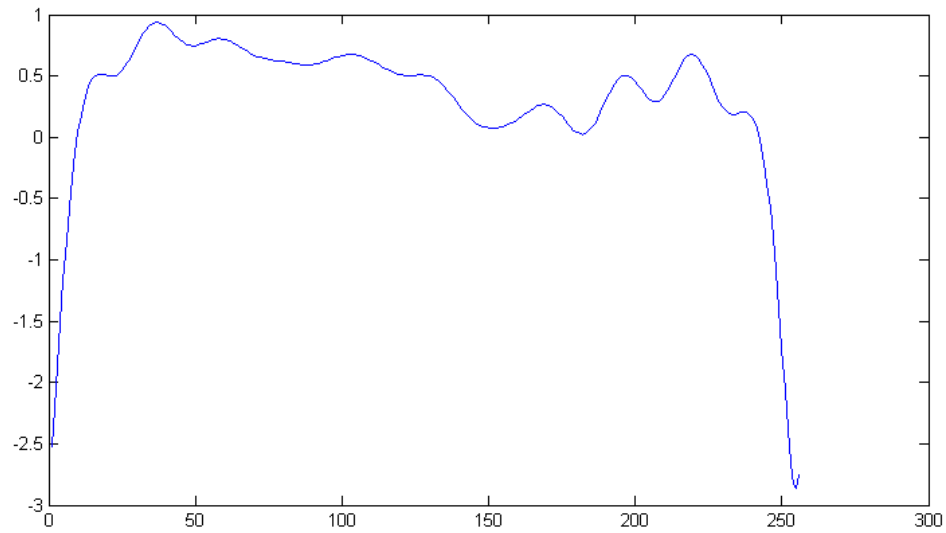


Figure 32. Channel A frequency response

### CHANNEL B

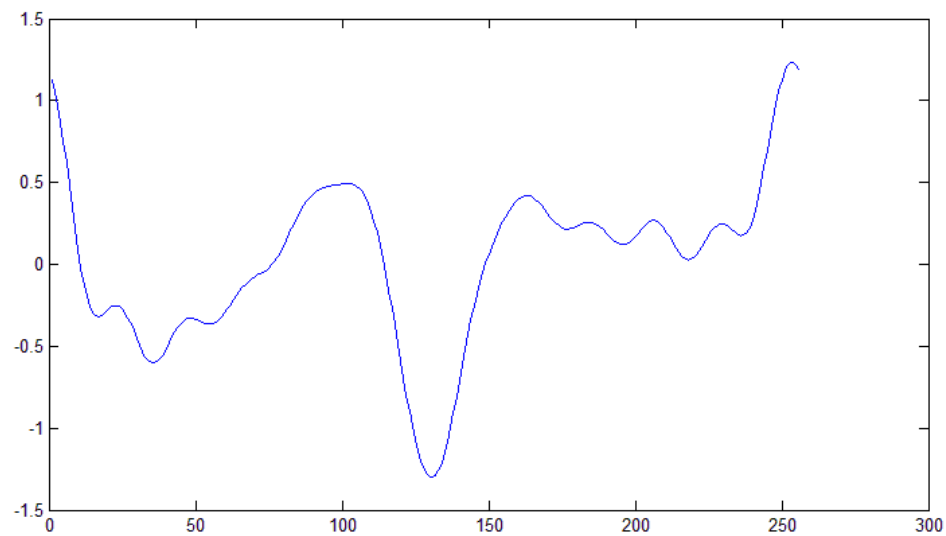


Figure 33. Channel B frequency response

It can be shown that the main difference between both channels is that Channel B is more frequency selective than Channel A which is more constant.

## **Equalization**

As it has been said in previous chapters, in this project it will be simulated to different kinds of equalization methods: Zero-Forcing and MMSE. Both methods are widely used in Frequency Domain Equalization and do not require of a high computational cost.

The following diagrams show the blocks that form each of the equalizers.

### ***Zero-Forcing $G=2$***

The following diagram shows the Zero Forcing equalizer module taking into account two repetitions of the CES:

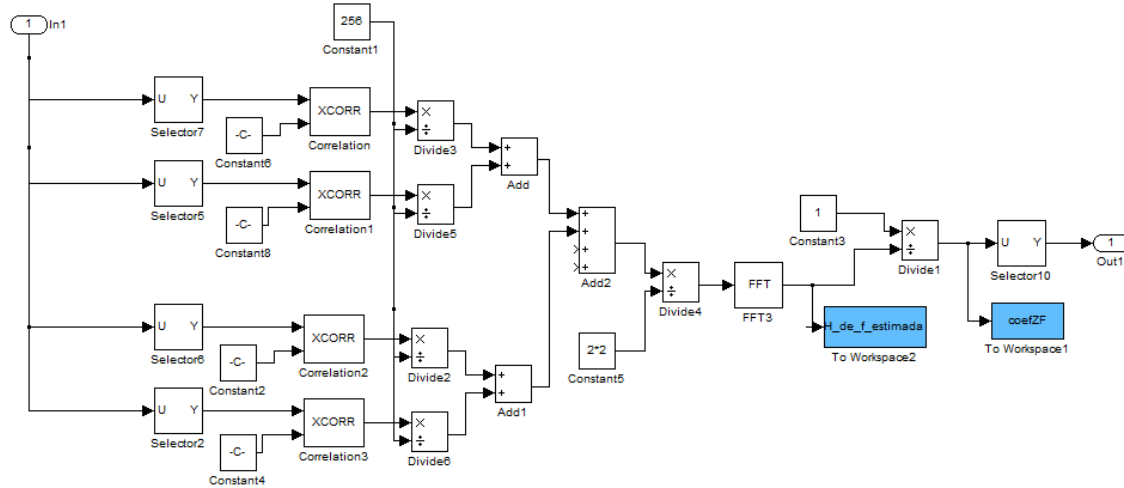


**Figure 34. Zero Forcing Equalizer with two CES repetitions**

To perform the equalization, it shall take into account the properties of Golay sequences.

Thus, each CES is composed of a sequence part A and B which are complementary between them. Next, these sequences are added and divided by two, as it can be shown in the previous figure. Later, the Fourier transform is applied and it can be obtained the estimated impulse response based on the number of repetitions of CES that will be used. Finally, the equalizer channel function  $E(f)$  or Zero-forcing coefficients  $C[k]$  is obtained, which in this case corresponds to the inverse of the estimated  $H[k]$ .

It is necessary to point that although the diagram presented before only takes into account two repetitions of CES to make the estimation of the channel impulse response, the simulations results consider as many repetitions of CES as are defined in the Standard 802.15.3c. This is done to minimize the error derived from each of the separate estimations and to obtain an average value as close to the real  $H(f)$  as possible.

### ***Minimum Mean Square Error $G=2$***

The following diagram shows the MMSE equalization module considering two repetitions of CES:

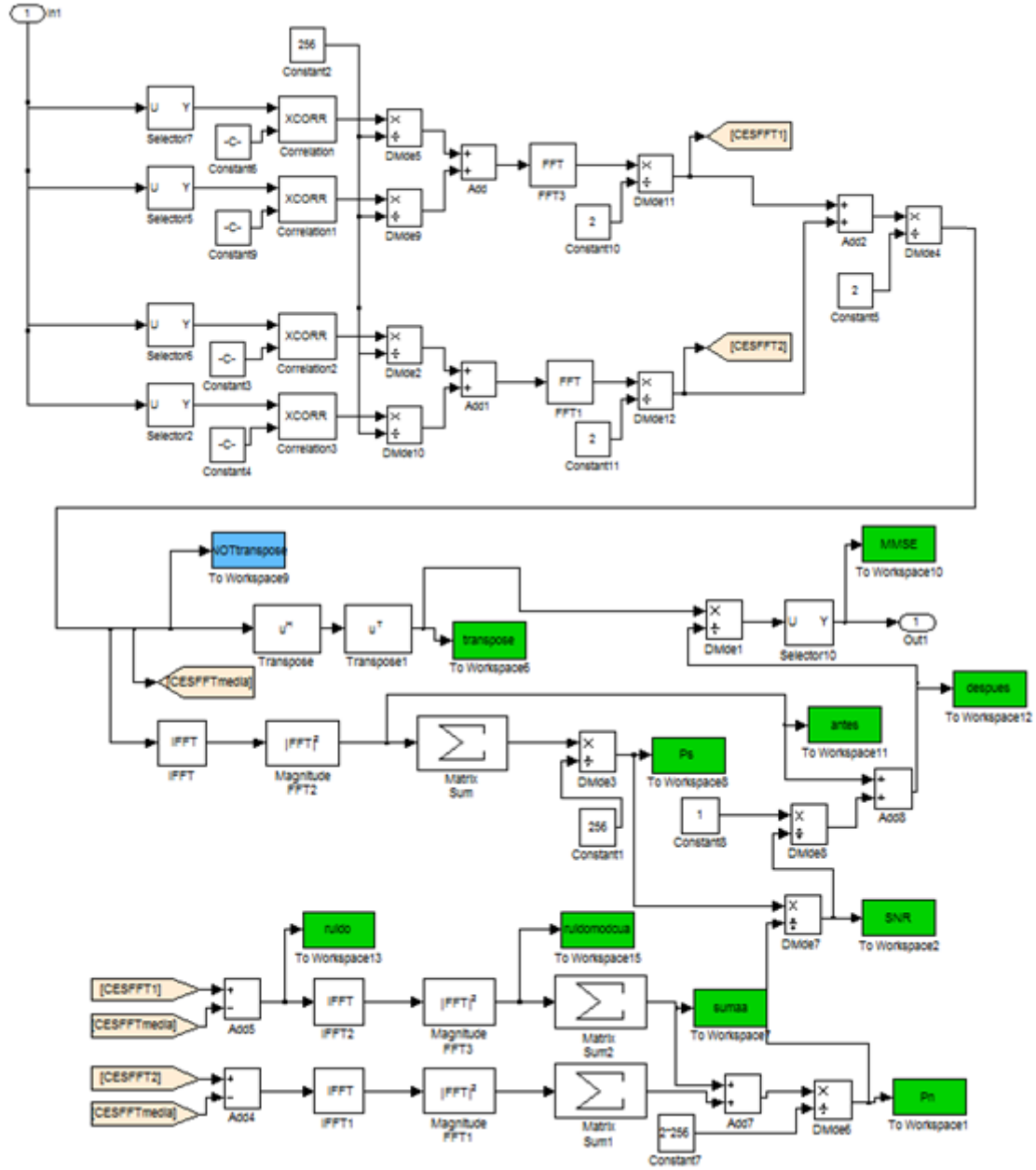


Figure 35. MMSE Equalizer with two CES repetitions

As in Zero-Forcing, for MMSE equalization will be taken into account the Golay sequences properties. Moreover, in this case the estimated channel frequency response  $H[k]$  is obtained in the same way as in the Zero-Forcing Equalizer; however MMSE Equalization method also includes a signal to noise ratio (SNR) estimation of the channel in order to improve the performance of the whole equalization. To estimate the SNR it will be calculated, on the one hand the power of the useful signal ( $P_s$ ) and on the other hand the noise power ( $P_n$ ). Then, both powers are compared in order to obtain SNR estimation. Finally the equalizer channel function  $E(f)$  or MMSE coefficients  $C[k]$  is obtained by using the following relation:

$$C[k] = \frac{H[k]^*}{|H[k]|^2 + 1/\eta}$$

Being  $\eta$  the estimated Signal-to-Noise ratio (SNR) and  $H[k]^*$  the conjugate transpose of  $H[k]$ .

It is also remarkable that just like in the Zero-Forcing diagram, the MMSE diagram presented before only takes into account two repetitions of CES. Nevertheless to carry out simulations all repetitions of CES have been considered. Furthermore, in this case CES repetitions also affects to SNR estimation, making it better in both ways (SNR and  $H[k]$  estimation).

## 5.2. Simulation Results

This section describes the obtained equalization results based on the two different propagation scenarios to be analyzed (channel 1 and 2). Considering all the default parameters defined before, the following tests will analyze both propagation channels taking into account: the estimated impulse response, the used equalization method, the different modulations schemes supported by the standard (BPSQ, QPSK, 8-PSK and 16-QAM), and the signal to noise normalized level per bit ( $E_b/N_0$ ).

It should be noted that all following figures on this section have been represented in the frequency domain mainly because Single Carrier equalization is performed in this domain and it is also easier to depict than in time domain.

### **Channel A**

#### **Original Channel frequency response $H[k]$**

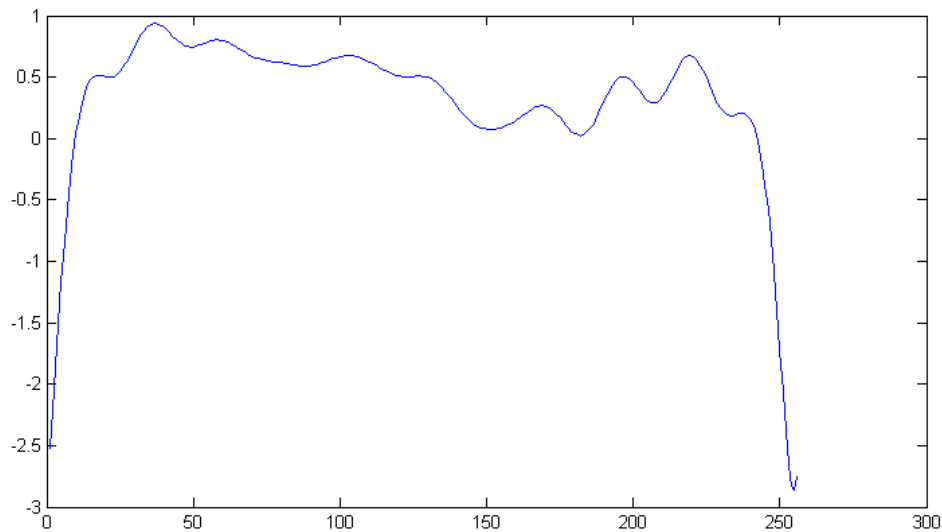
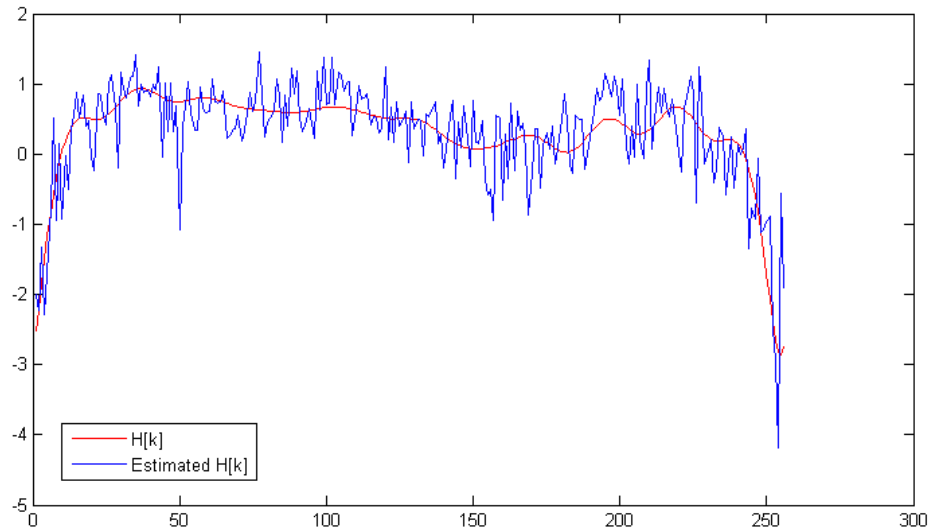


Figure 36. Channel A: Real channel frequency response

**Original Channel frequency response  $H[k]$  VS Estimated Channel frequency response  $H[k]$**

Applying  $E_b/N_o = 5 \text{ dB}$



**Figure 37. Channel A: Real channel frequency response VS Estimation with an  $E_b/N_o=5\text{dB}$**

As it can be seen, the estimated channel frequency response  $H[k]$  have certain resemblance to the original one, however there are some peak-to-peak errors up to 2 dB so it is necessary a better  $E_b/N_o$  on the channel in order to improve the estimated channel frequency response.

Applying  $E_b/N_o = 12 \text{ dB}$

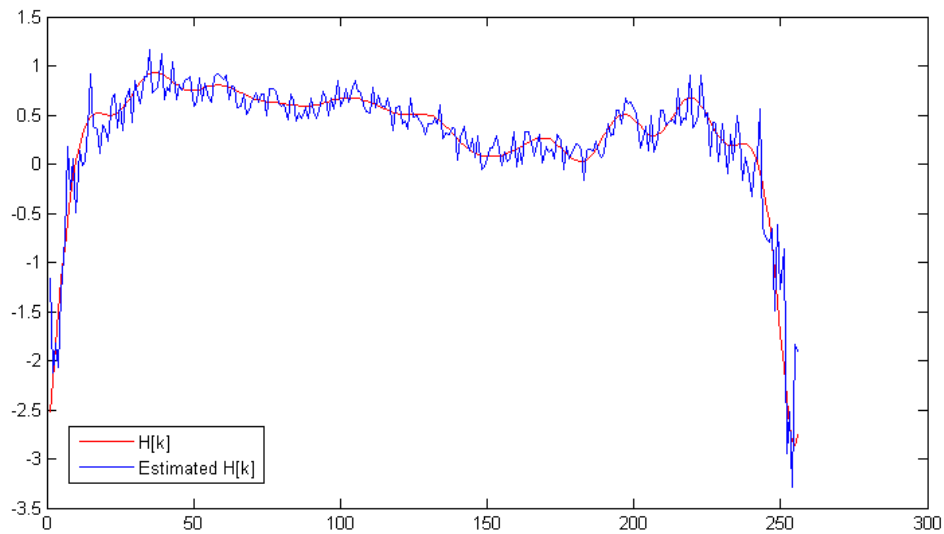


**Figure 38. Channel A: Real channel frequency response VS Estimation with an  $E_b/N_o=12\text{dB}$**

In this picture it can be seen how the higher  $E_b/N_0$  level of the channel, the better estimation of the channel frequency response, to the point of getting almost a frequency response equal to the original one if the  $E_b/N_0$  level is high enough depending on the channel.

### **Equalization**

Next, it will be shown the results of the different used equalization methods for comparison.

#### ➤ **Zero-Forcing Equalization VS Zero-Forcing Equalization using Golay Sequences**

To perform this comparison, it was taken into account a constant  $E_b/N_0$  of 5 dB, a low enough level to check the performance of one method over another when the channel does not have an acceptable quality in terms of  $E_b/N_0$ . It should be reminded that the best equalization performance is achieved when a flat frequency response is obtained at the system output.

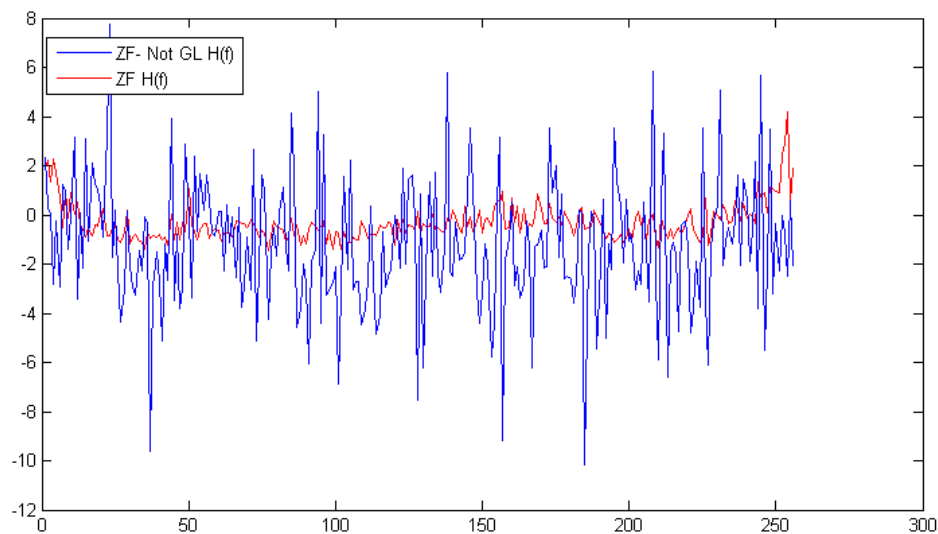


**Figure 39. Channel A: ZF Equalization VS ZF Equalization with Golay Sequences**

As it can be seen the error caused by the intersymbol interference ISI is reduced by the application of the Golay Complementary Sequences properties. Golay sequences reduce the miscalculation errors produced by ISI for channels with a low  $E_b/N_0$  level.

#### ➤ **Zero-Forcing Equalization VS MMSE Equalization (using GS in both cases)**

In this case an  $E_b/N_0$  equal to 5dB has been defined. In addition, the application of the Golay Sequences has been considered in both methods of equalization after verifying the improvement on the estimated channel frequency response at low  $E_b/N_0$  levels.

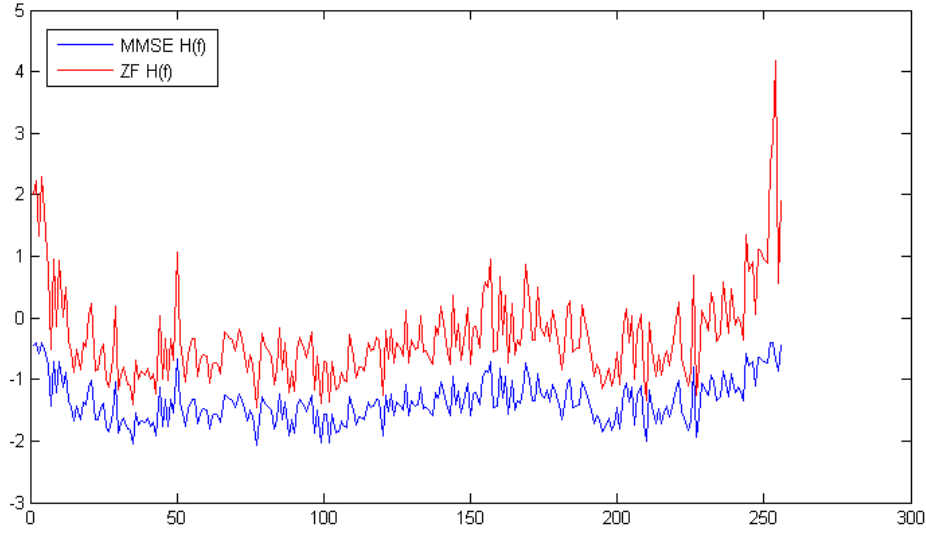


Figure 40. Channel A: ZF Equalization VS MMSE Equalization

As shown, the main difference between the two equalization methods is a significant reduction in the noise level by using MMSE equalization instead of Zero-Forcing equalization, thanks to the SNR estimation.

Moreover, the previous figure also shows how the Zero-Forcing equalizer has a worse response to spectral nulls (deep fading), amplifying strongly (infinity gain) those frequencies with a small value of the channel transfer function and enhancing the noise too. This is due to the form of the transfer function of the Zero-Forcing equalizer, which is  $E(f) = 1/H(f)$ .

### **Bit Error Rate performance for different modulations and equalization methods**

The following figures show the results that had been obtained for each equalization method in terms of Bit Error Rate performance. These tests are very useful because they allow seeing which equalization method works better in an intuitive way. The results had been realized for the most common modulations that are supported by the standard 802.15.3c (BPSK, QPSK and 16-QAM).

In all simulations, it has been taken into account: ZF without Golay Sequences, ZF with Golay Sequences and MMSE Equalization. To calculate the different BER performance for each equalizer it was necessary to apply different  $E_b/N_0$  to the channel in order to know its behaviour. It must be taken into account also that the total number of bits that have been used in order to obtain a correct BER calculation (stabilization period) is 65.536 bits.



### ➤ BPSK Modulation: ZF VS ZF using GS VS MMSE Equalization

In the following figure it can be seen the performance of every equalization method carried out using in this case a BPSK modulation. The results show that the equalization method with the worst performance is Zero-Forcing Equalization without applying the Golay Sequences properties, followed by Zero-Forcing using Golay Sequences and finally the best performance is done with MMSE Equalization. In fact, this performance is repeated for each modulation that has been tested and it is also the expected behaviour defined in theory.

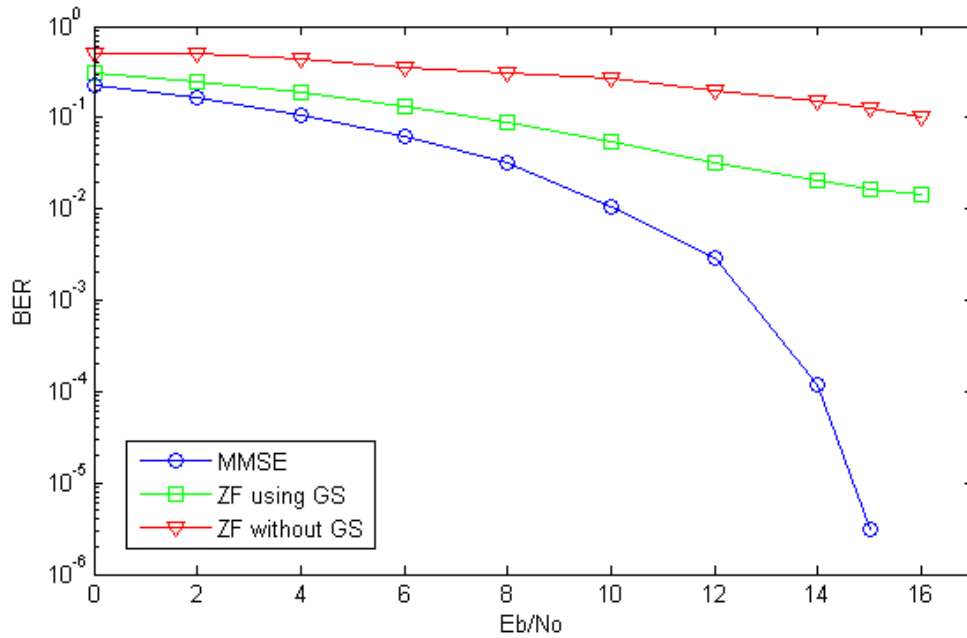


Figure 41. Channel A: BPSK modulation Equalization comparison

For BPSK modulation, the Zero-Forcing Equalization method has a BER of  $10^{-1}$  for a  $E_b/N_0$  equal to 16 dB, Zero-Forcing Equalization using GS reduces BER to a value around  $10^{-2}$  for  $E_b/N_0=16$  dB, and finally MMSE performance achieve a BER of  $3 \cdot 10^{-6}$  for a  $E_b/N_0$  of 15 dB.

### ➤ QPSK Modulation: ZF VS ZF using GS VS MMSE Equalization

In this case, the general performance is similar to that of the BPSK modulation, however MMSE Equalization has a higher BER for a  $E_b/N_0$  of 14 dB (around  $10^{-4}$ ) and it is necessary to achieve 16 dB in order to obtain BER levels lower than  $10^{-5}$ . Both Zero-Forcing Equalizations also have higher Bit Error Rate for each  $E_b/N_0$  compared to the BPSK modulation, nevertheless the BER values are between  $10^{-1}$  and  $10^{-2}$  which are actually worse than the MMSE equalization values.

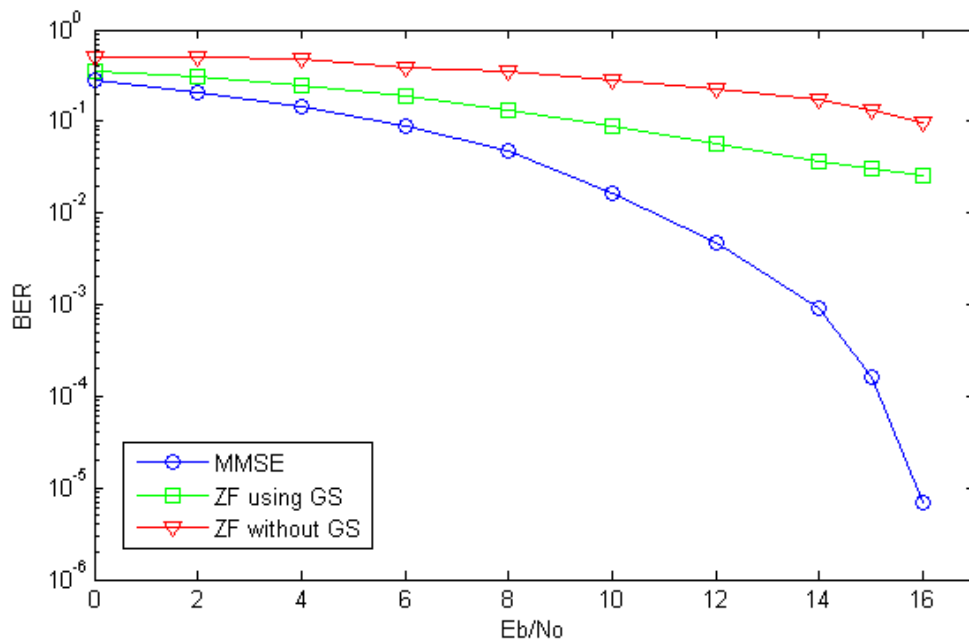


Figure 42. Channel A: QPSK modulation Equalization comparison

#### ➤ 16-QAM Modulation: ZF VS ZF using GS VS MMSE Equalization

As expected, using a “higher” modulation (more symbols per constellation) it is necessary to achieve higher  $E_b/N_0$  levels in order to differ between the different modulation symbols, and this causes a BER growth.

In this case, the best equalization method is also obtained with MMSE equalization. This time a  $E_b/N_0$  of 18 dB is required in order to obtain a BER of  $3 \cdot 10^{-5}$ . For ZF equalization and ZF equalization using GS, the BER performance is 0.2 and  $0.4 \cdot 10^{-1}$  respectively for  $E_b/N_0 = 18$  dB which is worse than with previous modulations.

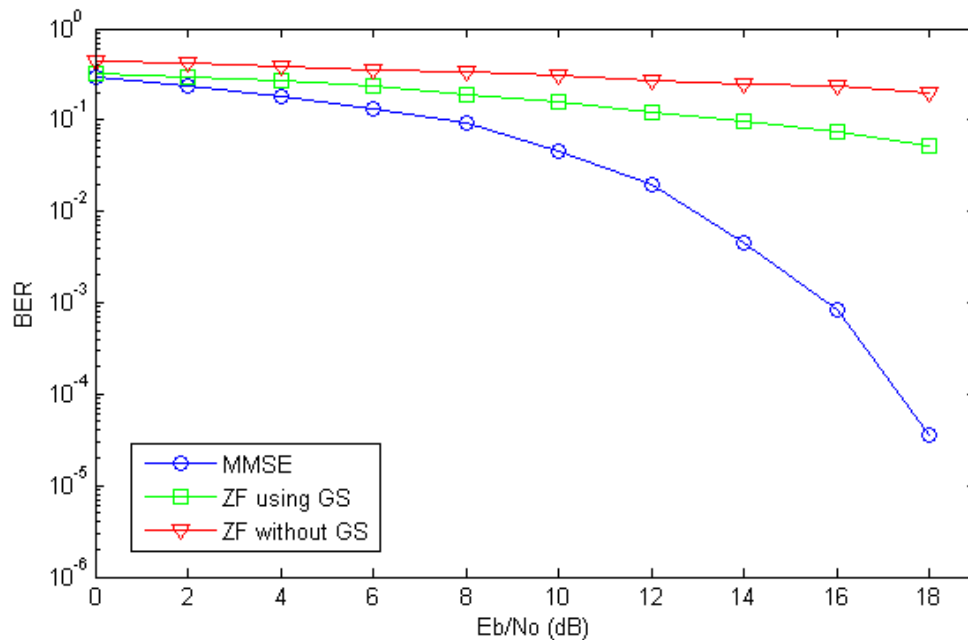


Figure 43. Channel A: 16-QAM modulation Equalization comparison

## **Channel B**

Original Channel frequency response  $H[k]$

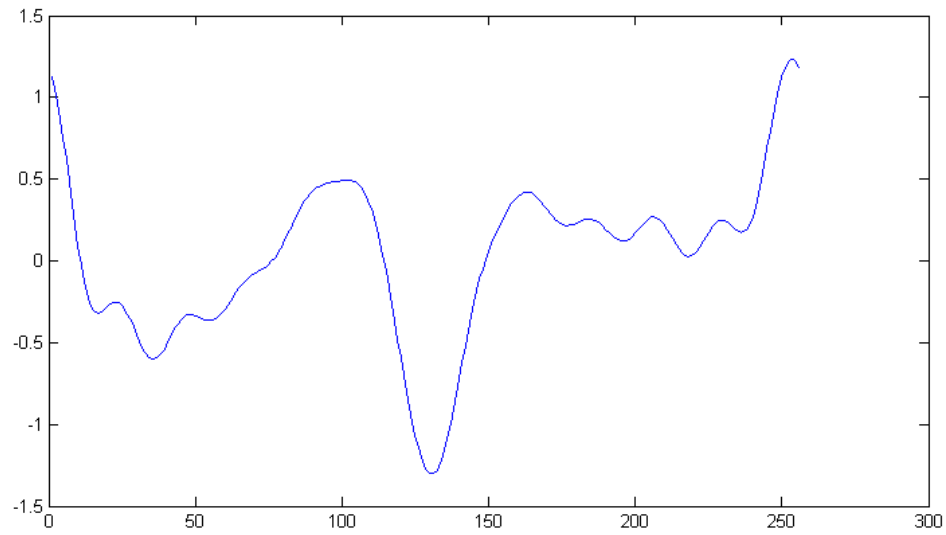


Figure 44. Channel B: Real channel frequency response

Original channel frequency response  $H[k]$  VS Estimated channel frequency response  $\hat{H}[k]$

Applying  $E_b/N_0 = 5 \text{ dB}$

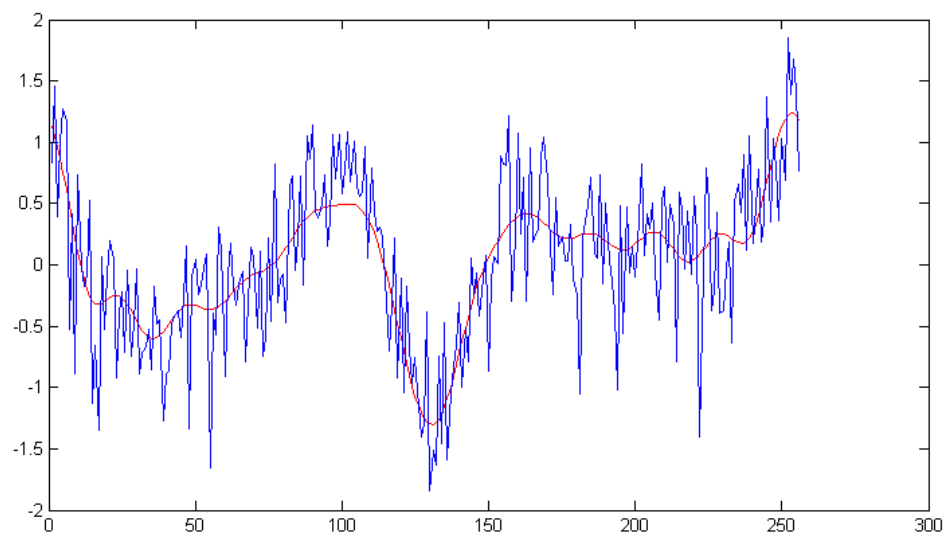


Figure 45. Channel B: Real channel frequency response VS Estimation with an  $E_b/N_0=5\text{dB}$

As it can be seen, the estimated channel frequency response  $\hat{H}[k]$  have certain resemblance to the original one, however there are some peak-to-peak errors up to 2 dB so it is necessary a better  $E_b/N_0$  on the channel in order to improve the estimated channel frequency response.

Applying  $E_b/N_o = 12 \text{ dB}$

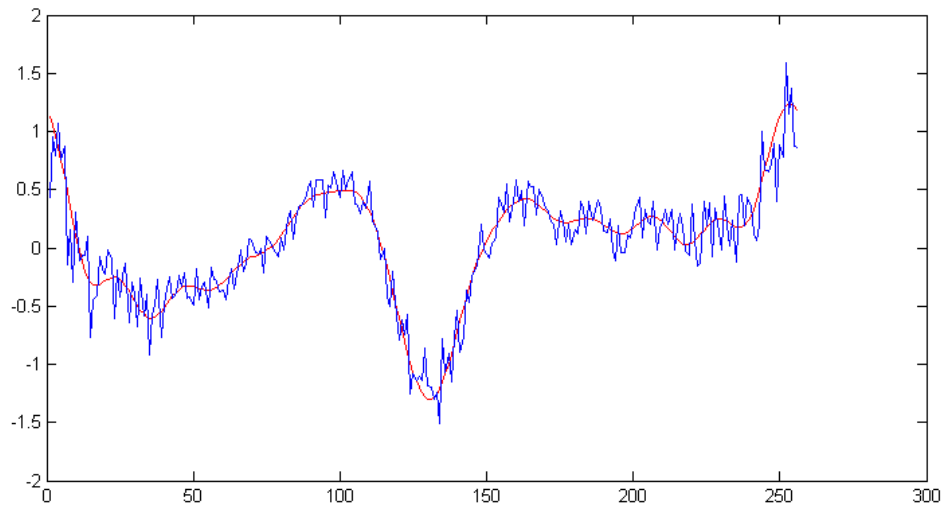


Figure 46. Channel B: Real channel frequency response VS Estimation with an  $E_b/N_o=12\text{dB}$

### Equalization

Next, it will be shown the results of the different used equalization methods in channel B for comparison.

#### ➤ Zero-Forcing Equalization VS Zero-Forcing Equalization using Golay Sequences

Exactly as in channel A, to perform this comparison it was considered a  $E_b/N_o = 5 \text{ dB}$ , a low enough level to check the performance of one method over another when the channel does not have an acceptable quality in terms of  $E_b/N_o$ .

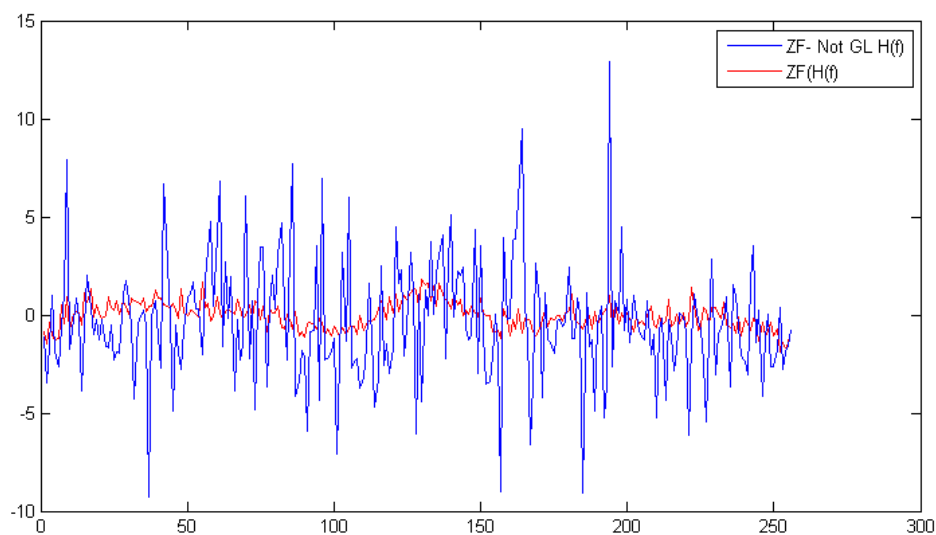
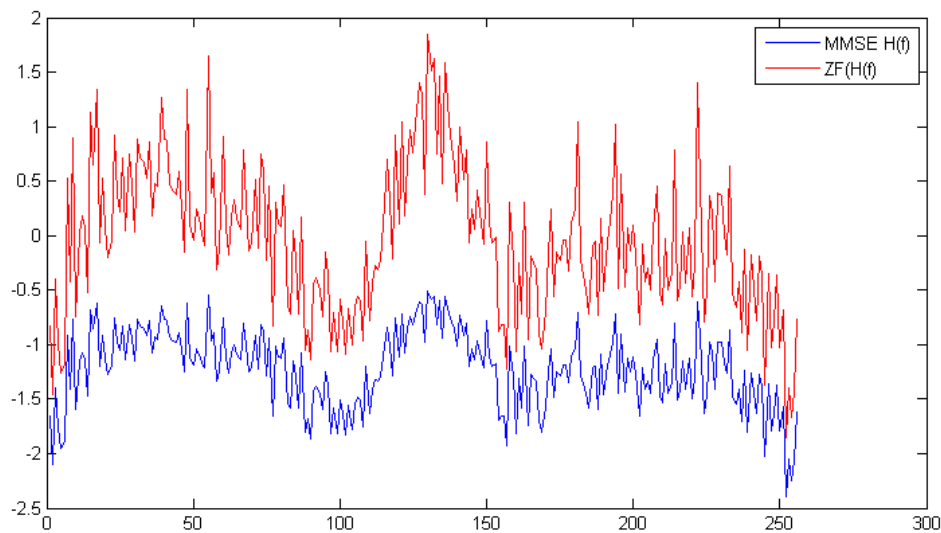


Figure 47. Channel B: ZF Equalization VS ZF Equalization with Golay Sequences

As in previous channel, thanks to Golay Complementary Sequences properties it can be reduce the miscalculation errors produced in a Zero Forcing Equalization, avoiding error peaks that can reach almost 15 dB. Also, it can be deduced comparing both channels Zero Forcing Equalizations that Channel A has better general performance (less propagation effects) than Channel B, since error peaks in Channel A are greater than in Channel B, which implies that it will be needed a higher  $E_b/N_0$  level to obtain a similar Bit Error Rate to thus of Channel A with lower  $E_b/N_0$ .

➤ **Zero-Forcing Equalization VS MMSE Equalization (using GS in both cases)**

In this case, an  $E_b/N_0$  equal to 5dB has been defined, too.



**Figure 48. Channel B: ZF Equalization VS MMSE Equalization**

As in previous channel, the main difference between the two equalization methods is the reduction thanks to the SNR estimation that is taken into account for MMSE equalization and not in Zero-Forcing method.

Moreover, in Zero-Forcing all spectral peaks are amplified strongly producing more errors in reception than data processed with MMSE method.

**Bit Error Rate performance for different modulations and equalization methods**

Next, it will be shown the results of each equalization method in terms of Bit Error Rate performance. The results had been realized for BPSK, QPSK and 16-QAM modulations.

➤ **BPSK Modulation: ZF VS ZF using GS VS MMSE Equalization**

The general performance in Channel B is really similar to that of Channel A as would be seen. In this case the results show that the equalization method with the worst performance is ZF Equalization without GS properties with a BER value higher than  $10^{-1}$  for  $E_b/N_0$  equal to 16 dB, followed by ZF using GS and MMSE which is the best performance with a BER value of  $7.2 \cdot 10^{-6}$  for  $E_b/N_0$  equal to 15 dB.

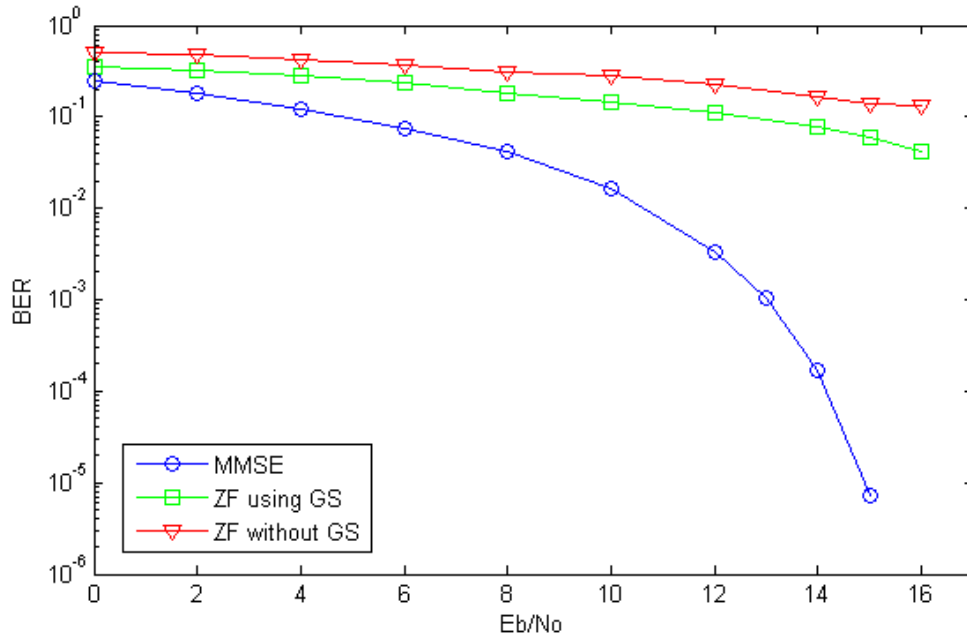


Figure 49. Channel B: BPSK modulation Equalization comparison

➤ **QPSK Modulation: ZF VS ZF using GS VS MMSE Equalization**

As in previous channel, QPSK modulation in channel B requires higher  $E_b/N_0$  in order to obtain less Bit Error Rate due to digital modulation scheme. As can be seen, MMSE Equalization has the best performance (around  $10^{-5}$  BER) for an  $E_b/N_0$  equal to 16 dB, meanwhile ZF and ZF-GS Equalization has higher BER than  $10^{-2}$  for the same  $E_b/N_0$ , which is significantly worse than MMSE Equalization.

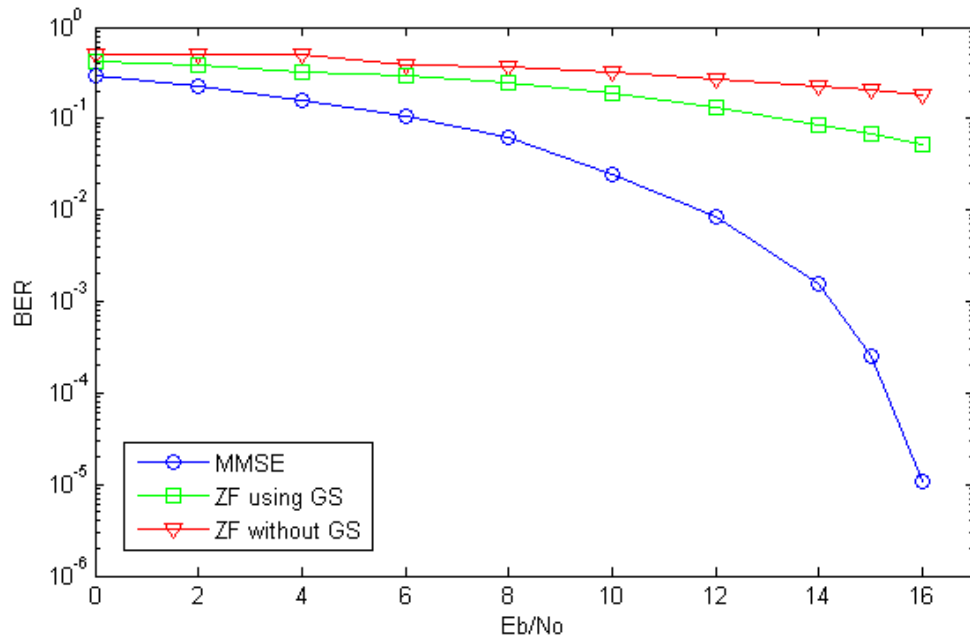


Figure 50. Channel B: QPSK modulation Equalization comparison

#### ➤ 16-QAM Modulation: ZF VS ZF using GS VS MMSE Equalization

In this case, using a 16-QAM modulation it is necessary to achieve higher  $E_b/N_0$  levels in order to improve the Bit Error Rate. This time, MMSE equalization has a BER of  $7.3 \cdot 10^{-5}$  for a required  $E_b/N_0$  of 18 dB, which is significantly higher than the 15 dB needed to obtain a better performance in modulations such as BPSK or QPSK. Finally ZF equalization and ZF equalization using GS has the worst performance of all test carried out with a BER value of 0.28 and 0.15 respectively for a  $E_b/N_0=18$  dB.

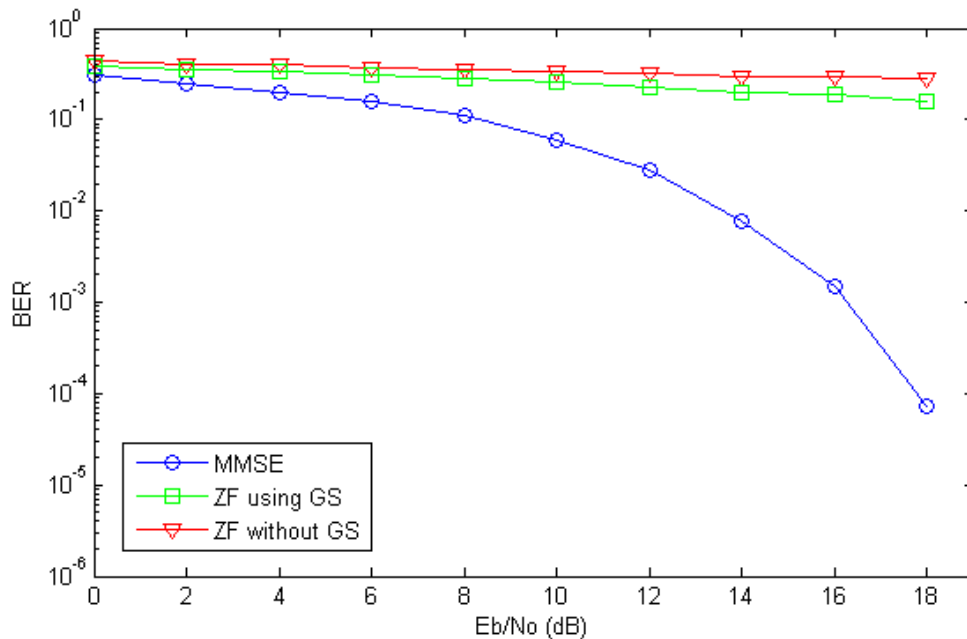


Figure 51. Channel B: 16-QAM modulation Equalization comparison

## Conclusions

During the theoretical study of this final thesis it has been denoted that there are a lot of aspects that affect the high speed wireless transmission producing undesirable effects that pose a problem during transmission. Some of them are multipath propagation effects, such as fading or intersymbol interference, frequency selectivity and linear time variant systems; however it can be avoided with a properly estimation and channel equalization.

Moreover, taking into account the IEEE 802.15.3c standard for high data rates transmissions in short-range indoor applications by using 60-GHz frequency band, basically there are two candidate PHY techniques under consideration for multi-Gbps WPAN: Orthogonal frequency division multiplexing (OFDM) and single-carrier transmission (SC); depending on each physical layer mode.

In this stage of the project only single carrier technology has been taking into account, leaving OFDM for future simulations, nevertheless both technologies have to be equalized in the frequency domain (FDE) according to the standard.

Single Carrier frequency domain equalization (SC-FDE), make inter-symbol interference (ISI) caused by multi-path fading channel easier to remove than in time domain equalization. However, Golay complementary sequences have been also taken into account to estimate channel frequency response and SNR. The prominent feature of these sequences is that the sum auto-correlation has a unique peak and zero sidelobe, which can effectively remove ISI to improve the channel estimation accuracy as have been demonstrated into the carried simulations.

Frequency Domain Equalization has been developed by using two different equalization methods: Zero Forcing (ZF) and Minimum Mean Square Error (MMSE). As have been demonstrated during simulations, MMSE-FDE has much better performance than ZF-FDE, however it needs to know signal-to-noise ratio (SNR). This conclusion is repeated for every modulation that had been analyzed: BPSK, QPSK and 16-QAM. Also worth noting is the important trade-off between Bit Error Rate (BER) and the  $E_b/N_0$  of the transmission channel that show the simulation results, or in other words, the relation between the normalized channel SNR improvement and the reduction of BER.



Finally, the results show that by using a reasonable number of channel estimation sequences (CES), the MMSE-FDE based on estimated SNR has lower performance degradation in comparison with ZF-FDE. In BER terms, the difference between both methods according to simulations could be from a  $\text{BER}=10^{-1}$  achieved with a ZF-FDE method up to  $\text{BER}=10^{-5}$  obtained with a MMSE-FDE performance with enough channel Eb/No quality (that also depends on the modulation scheme). Thus, it can be concluded that MMSE-FDE (aided by SNR estimation) in Single Carrier technology is very promising for realizing data rates of multi-Gbps in WPAN.

## References

- [1] IEEE 802.15.3c “Wireless Medium Access Control (MAC) and Physical Layer (PHY) Specifications for High Rate Wireless Personal Area Networks (WPANS)”
- [2] A. F. Molisch, “Wireless Communications”
- [3] M. Lei and Y. Huang, “CFR and SNR Estimation Based on Complementary Golay Sequences for Single Carrier Block Transmission in 60GHz PAN” in 2009.
- [4] J. Tubbax, B. Côme, L. Van der Perre, L. Deneire, S. Donnay and M. Engels, “OFDM versus Single Carrier with Cyclic Prefix, a system-based comparison” in 2001
- [5] J. van de Beek, O. Edfors, M. Sandell, S. Kate Wilson and P. O. Börjesson, “On Channel Estimation in OFDM systems”.
- [6] E. Martinez and Y. Shen, “Channel Estimation in OFDM Systems”.
- [7] H. Sari, G. Karam and I. Jeanclaude, “Transmission Techniques for Digital Terrestrial TV Broadcasting” in February 1995.
- [8] B. Muquet, M. de Courville and P. Duhamel, “Subspace-Based Blind and Semi-Blind Channel Estimation for OFDM Systems” in July 2002.
- [9] Y. Li, L. J. Cimini and N. R. Sollenberger, “Robust Channel Estimation for OFDM System with Rapid Dispersive Fading Channels” in July 1998.
- [10] J. Tubbax, B. Come, L. Van der Perre, L. Deneire, S. Donnay and M. Engels “OFDM versus Single Carrier with Cyclic Prefix: a system-based comparison” in 2001.
- [11] O. Edfors, M. Sandell, J. Van de Beek, S. Kate Wilson and P.O. Börjesson “OFDM Channel Estimation by Singular Value Decomposition” in July 1998.
- [12] M. Lei, I. Lakkis, H. Harada and S. Kato “MMSE-FDE based on estimated SNR for Single-Carrier Block Transmission (SCBT) in Multi-Gbps WPAN” in 2008.
- [13] M. Lei, I. Lakkis, H. Harada and S. Kato “MMSE-FDE based on estimated SNR for Single-Carrier Block Transmission (SCBT) in Multi-Gbps WPAN” in 2008.